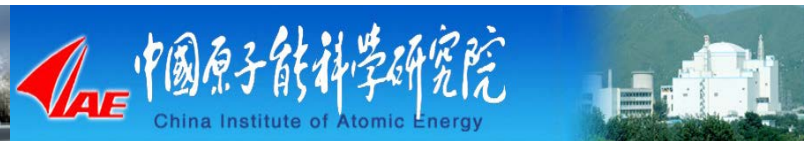




# ***Nuclear Data Activities in China***

**GE Zhigang 葛智刚**

**China Nuclear Data Center(CNDC)  
China Committee of Nuclear Data(CCND)  
China Institute of Atomic Energy(CIAE)  
P.O.Box 275-41,Beijing 102413, P.R.China  
E-Mail:gezg@ciae.ac.cn**





- 1.Introduction***
- 2.Activities of Nuclear Data Evaluation***
- 3.Activities of Nuclear Data Measurement***
- 4.Conclusions***



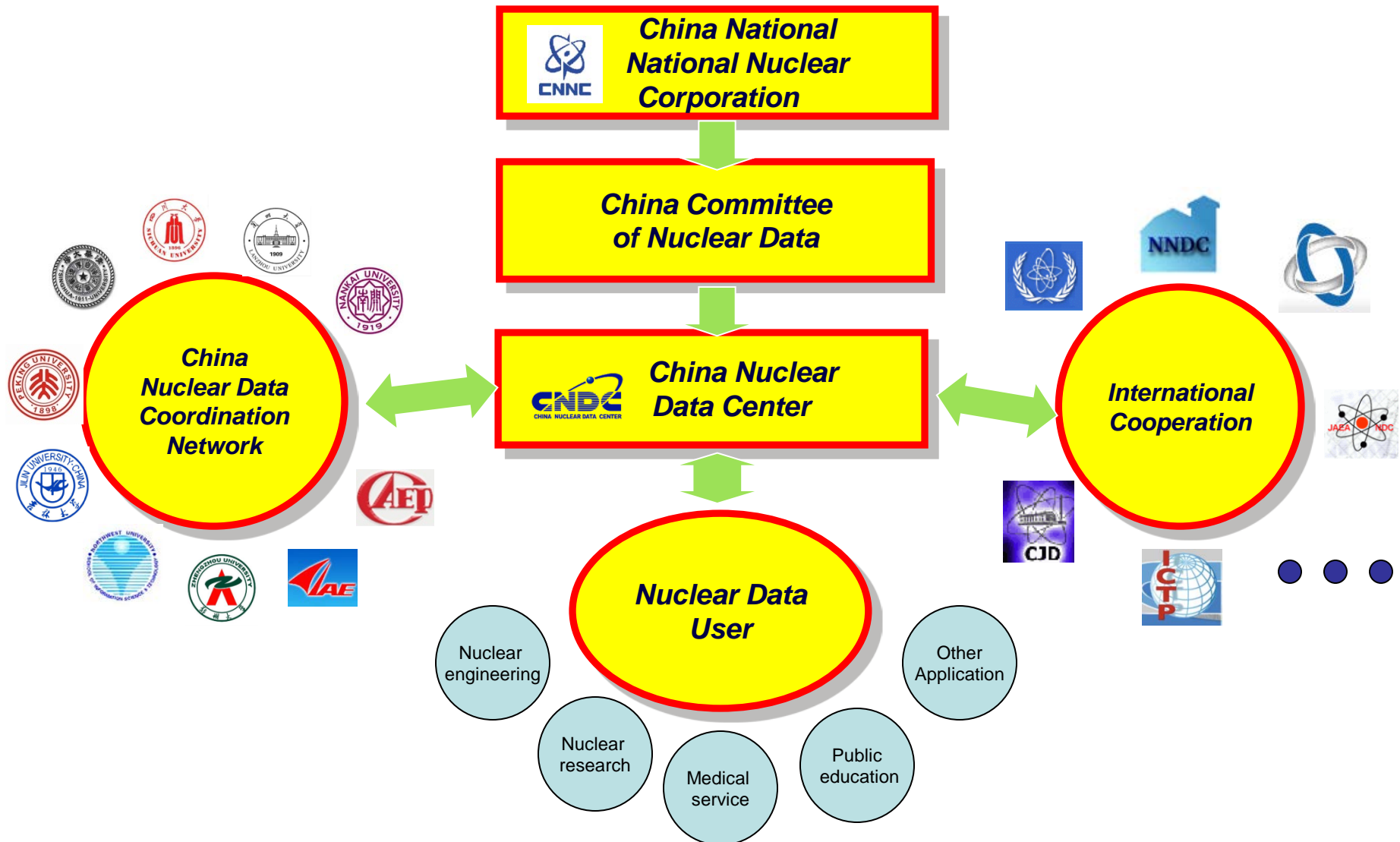
# 1. Introduction

The mainly nuclear data measurement activities in China are carried out at China Institute of Atomic Energy(CIAE) and China Nuclear Data Coordination Network(CNDCN). About 10 institutions and universities in China are involved CNDCN.





## The Chinese Nuclear Data Activity Structure





## Information of CNDC

### ***CNDC consists of the four units + an office:***

<i>Evaluation Unit</i>	<i>Head: Dr. Huang Xiaolong</i>	<i>3 official staff</i>
<i>Theory Unit</i>	<i>Head: Dr. Ge Zhigang</i>	<i>8 official staff</i>
<i>Macroscopic Data Unit</i>	<i>Head: Dr. Liu Ping</i>	<i>5 official staff</i>
<i>Data Library Unit</i>	<i>Head: Dr. Shu Nengchuan</i>	<i>5 official staff</i>
<i>Secretary Office</i>		<i>2 official staff</i>

### ***Director of CNDC:***

***Dr. Ge Zhigang***

***22 official staff and 5 technical support experts(senior) working at the CNDC and 4 graduate students and 3 Ph.D students are studying at CNDC.***





## **2. Activities of Nuclear Data Evaluation**

### ***2.1 Introduction of CENDL-3.1***

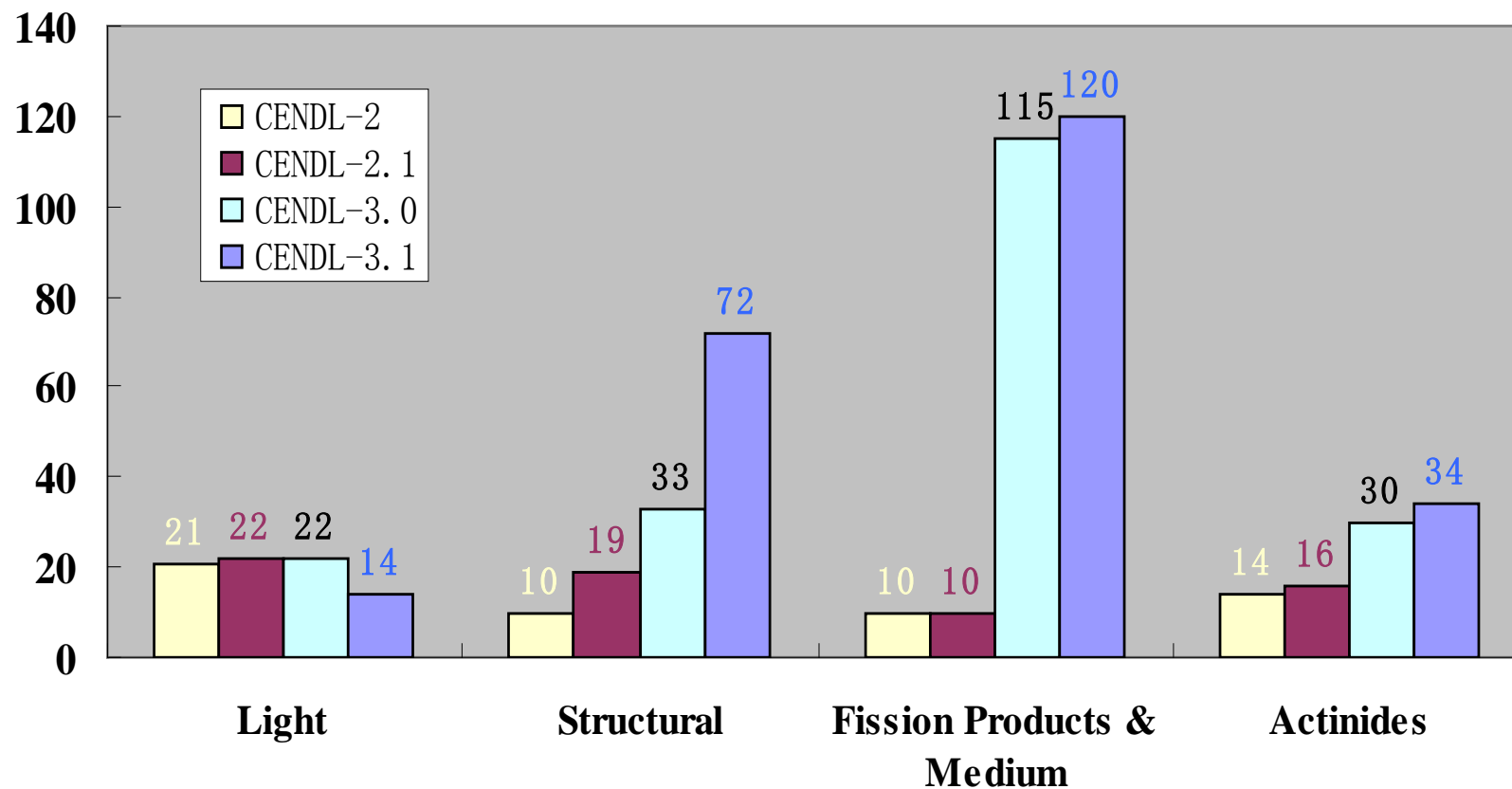
CENDL-3.1 is a general purpose evaluated nuclear data file, which contains the results of the nuclear data evaluations and measurement activities in recent years in China. CENDL-3.1 contains the evaluated data files for reactions with incident neutrons on almost 240 nuclides (see Table 2-1), among them, 173 nuclides are newly evaluated, and 37 nuclides are taken from previous vision of CENDL.

## Table 2-1 The nuclides of CENDL-3.1

<i>Nucl.</i>	<i>Content of Nuclei</i>
<i>Light Nuclei</i>	${}^1\text{H}, {}^3\text{He}, {}^6\text{Li}, {}^9\text{Be}, {}^{10,11}\text{B}, {}^{12}\text{C}, {}^{14}\text{N}, {}^{16}\text{O}, {}^{19}\text{F}$
<i>Structural Materials</i>	${}^{23}\text{Na}, {}^{24-26}\text{Mg}, {}^{27}\text{Al}, {}^{28-30}\text{Si}, {}^{31}\text{P}, {}^0\text{S}, {}^0\text{Cl}, {}^0\text{K}, {}^0\text{Ca}, {}^{46-50}\text{Ti}, {}^0\text{V}, {}^{50,52-54}\text{Cr}, {}^{55}\text{Mn}, {}^{54,56-58}\text{Fe}, {}^{59}\text{Co}, {}^{58,60-62,64}\text{Ni}, {}^{63,65}\text{Cu}, {}^0\text{Zn}, {}^0\text{Ge}, {}^{90-92,94,96}\text{Zr}, {}^{92,94-98,100}\text{Mo}, {}^{107,109}\text{Ag}, {}^0\text{Cd}, {}^0\text{Sn}, {}^{174,176-180}\text{Hf}, {}^{181}\text{Ta}, {}^0\text{W}, {}^{197}\text{Au}, {}^0\text{Hg}, {}^0\text{Tl}, {}^{204,206-208}\text{Pb}, {}^{209}\text{Bi}$
<i>Fission Products &amp; Medium Elements</i>	${}^{69,71}\text{Ga}, {}^{70-78}\text{Ge}, {}^{75,77,79}\text{As}, {}^{83-86}\text{Kr}, {}^{85,87}\text{Rb}, {}^{88-90}\text{Sr}, {}^{89,91}\text{Y}, {}^{93,95}\text{Zr}, {}^{93,95}\text{Nb}, {}^{99}\text{Tc}, {}^{99-105}\text{Ru}, {}^{103,105}\text{Rh}, {}^{105,108}\text{Pd}, {}^{113}\text{Cd}, {}^{113,115}\text{In}, {}^{112,114-120,122,124}\text{Sn}, {}^{121,123,125}\text{Sb}, {}^{130}\text{Te}, {}^{127,129,135}\text{I}, {}^{123,124,129,131,132,134-136}\text{Xe}, {}^{133-135,137}\text{Cs}, {}^{130,132,134-138}\text{Ba}, {}^{139}\text{La}, {}^{136,138,140-142,144}\text{Ce}, {}^{141}\text{Pr}, {}^{142-148,150}\text{Nd}, {}^{147,148,148\text{m},149}\text{Pm}, {}^{144,147-152,154}\text{Sm}, {}^{151,153-155}\text{Eu}, {}^{152,154-158,160}\text{Gd}, {}^{164}\text{Dy}$
<i>Actinides</i>	${}^{232}\text{Th}, {}^{232-241}\text{U}, {}^{236-239}\text{Np}, {}^{236-246}\text{Pu}, {}^{240-244,242\text{m}}\text{Am}, {}^{249}\text{Bk}, {}^{249}\text{Cf}$



## CONTENT OF CENDL- 3.1



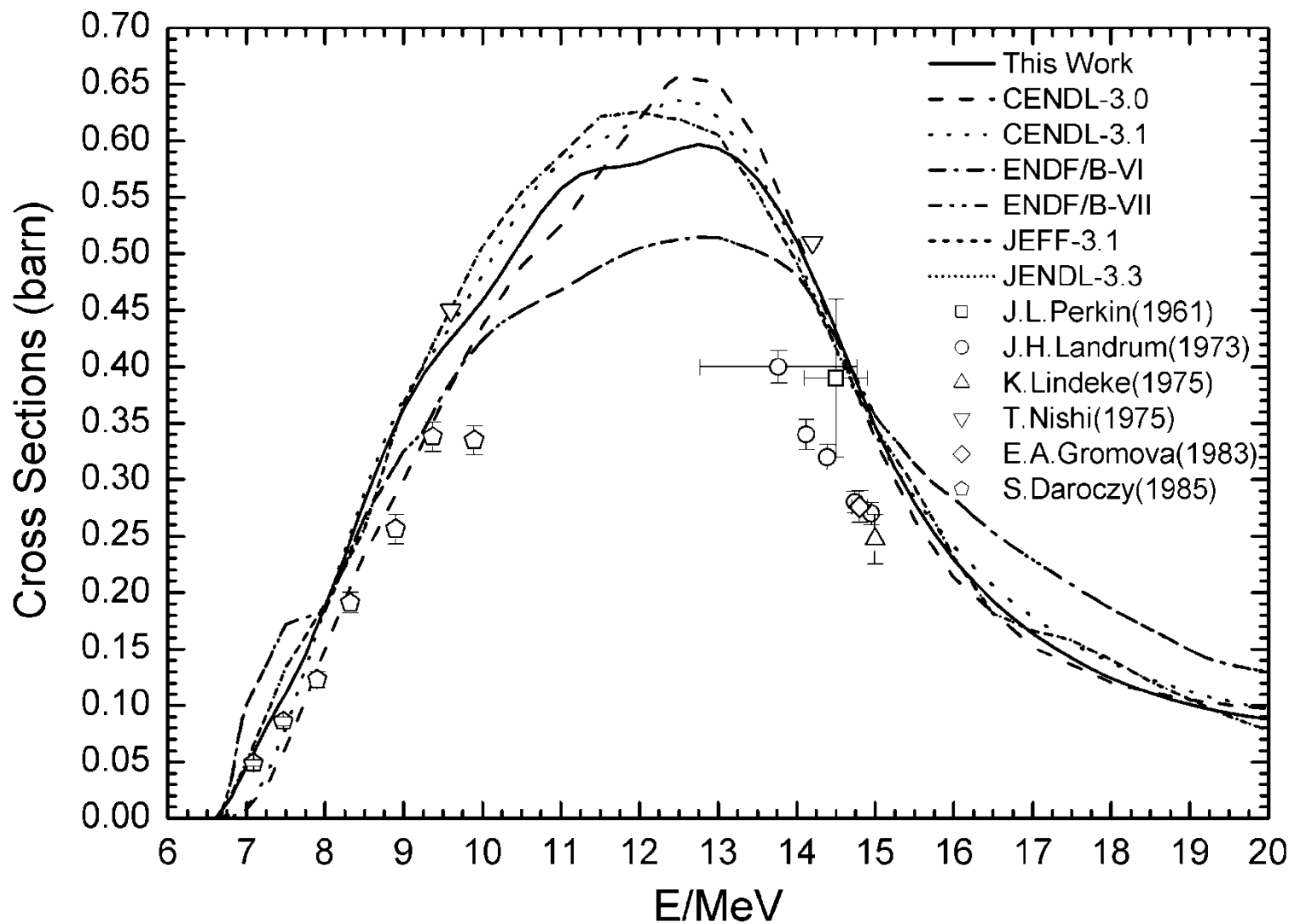




## 2.2 Status of CENDL-3.1

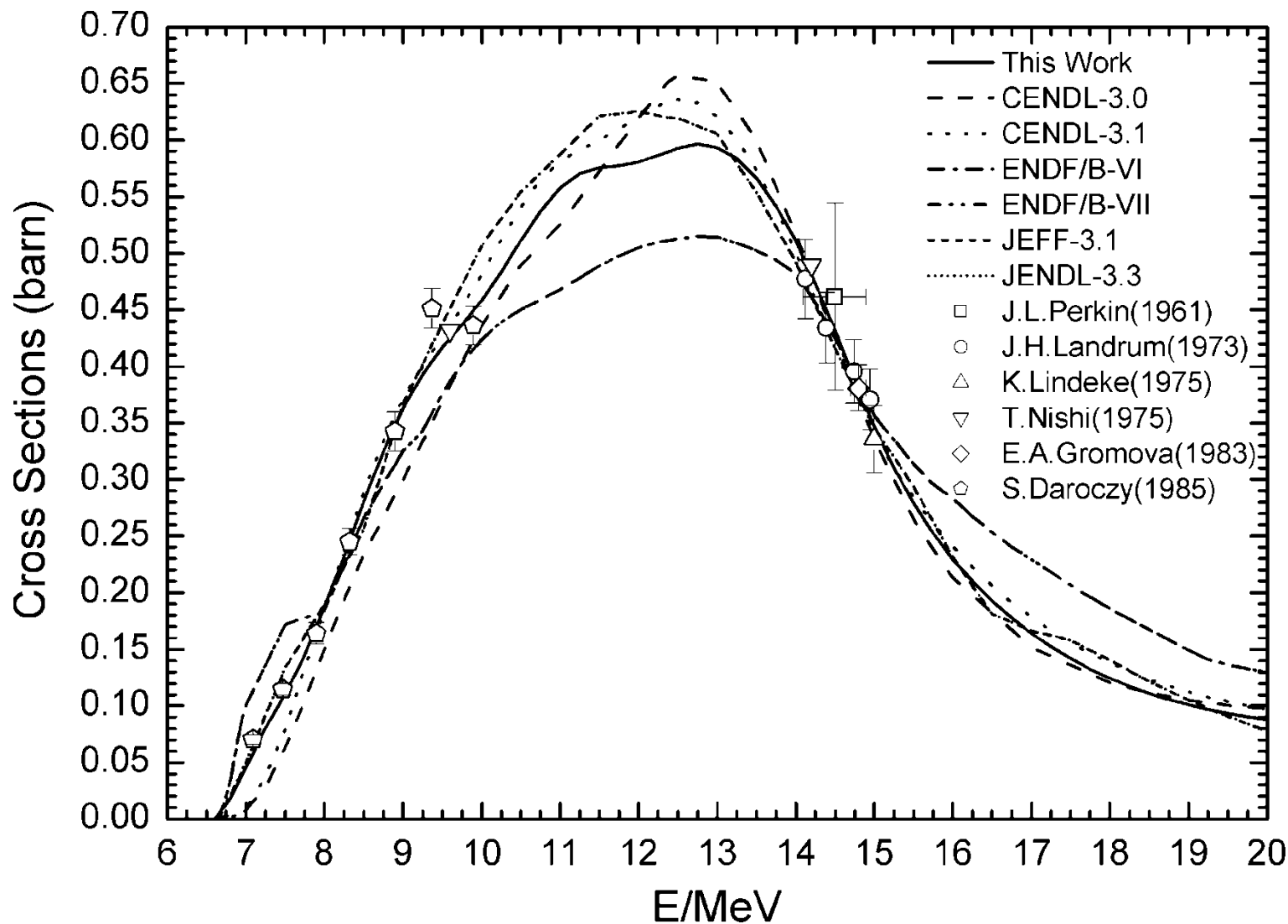
### Data Files Re-evaluation

According to the back feed from the benchmark testing and users, some data files (MT) of CENDL-3.1 were re-evaluated in recent two years. These nuclei including the actinides  $^{241}\text{Am}$ ,  $^{234,235}\text{U}$ ,  $^{237}\text{Np}$ ,  $^{233}\text{Th}$  and some structural materials  $^{54}\text{Fe}$ ,  $^{97}\text{Mo}$ ,  $^{186}\text{W}(\text{p},\text{n})$ ,  $(\text{p},2\text{n})$ ,  $^{208,207,206,204}\text{Pb}$  et al.



(a) Comparison with original measured data

Fig.2-1 Comparison of evaluated data with measured data for  $^{237}\text{Np}(n, 2n)$  reaction



(b) Comparison with corrected measurements

Fig.2-2 Comparison of evaluated data with measured data for  $^{237}\text{Np}(n, 2n)$  reaction

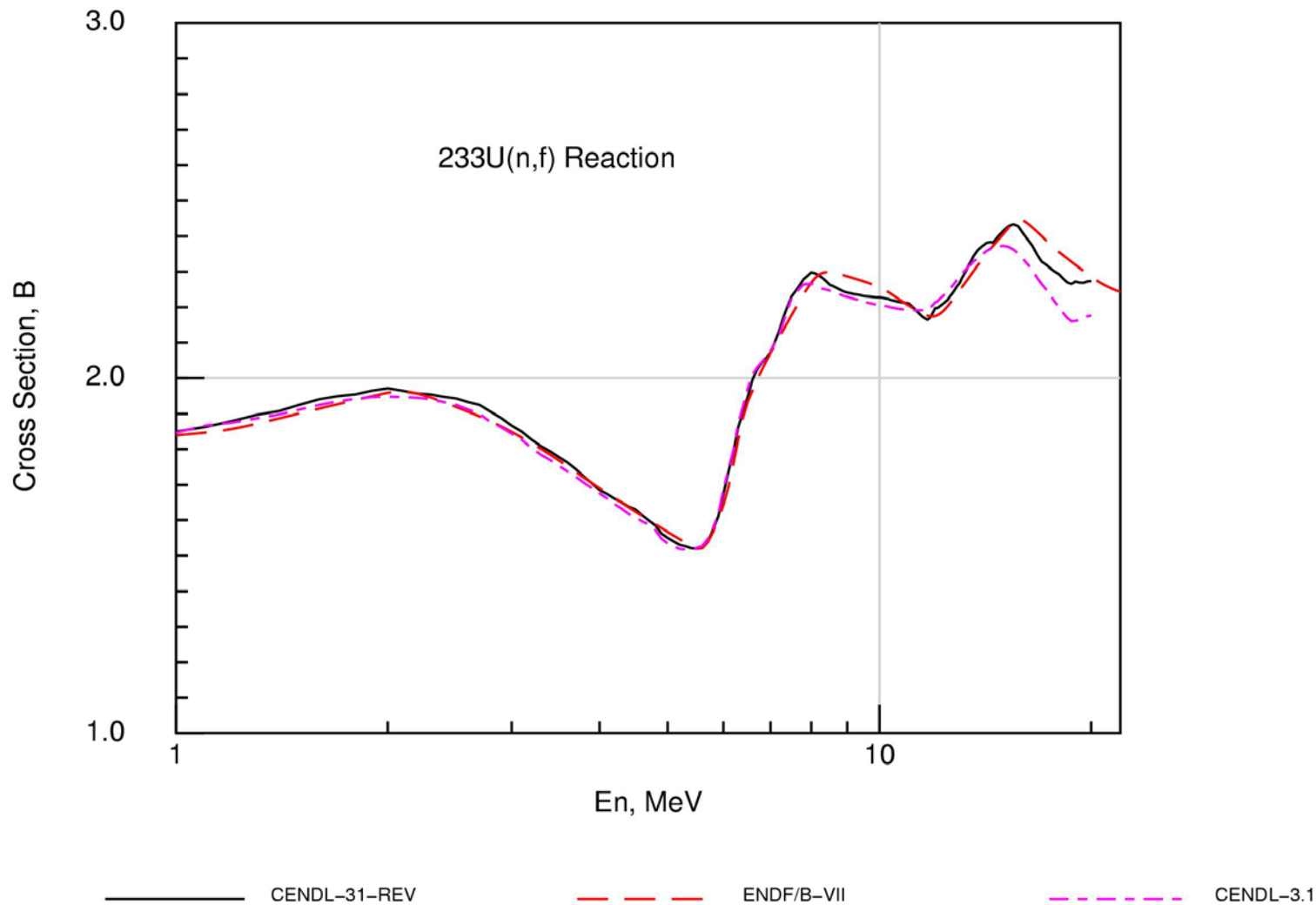


Fig. 2-3 Comparison of CENDL-31-REV, CENDL-31, ENDF/B-VII for  $^{233}\text{U}(n, f)$  Reaction



# **Data Benchmark Testing/Validation**

## ***Validation of Evaluated Data Library with CSEWG benchmarks***

Several Cross Section Evaluated Workgroup(CSEWG) benchmarks were selected for validation of evaluated data files. These cases cover fast and thermal energy spectrum. The calculated results of effective multiplication factor  $k_{\text{eff}}$  were compared with the experimental results.

Los Alamos National Laboratory (LANL) benchmarks are including bare cores of highly-enriched  $^{235}\text{U}$  (Godiva),  $^{239}\text{Pu}$ (Jezebel) and  $^{233}\text{U}$ (Jezebel-23), which are selected for data testing. The Flattop series which include natural uranium reflector, such as Flattop-25, Flattop-Pu and Flattop-23 are adopted too. Also, investigations for the THOR assembly which has  $^{232}\text{Th}$  reflector and the Big-ten assembly are performed in this work. Some Pacific Northwest Laboratory(PNL) assemblies, solution and MOX fuel cases, and Oakridge National Laboratory assemblies were investigated too. The results are shown in table 2,3,4 and 5 respectively.

Criticality calculations were done by using Monte Carlo code MCNP4C. The ACE files were produced with nuclear data processing code NJOY99.259. For a single job, 10000 histories for 1000 active cycles were executed generally in parallel computer system. Estimated standard deviation in critical calculation was often below than 30pcm.



Table 2-2 Results of LANL sphere fast assemblies

Assembly	CENDL-3.1	ENDF/B-VII.0	JENDL-3.3	JENDL-4.0	Experiment	Error
Godiva	0.99999	0.99994	1.00277	0.99746	1.0004	0.0024
BIG TEN	0.99555	0.99467	0.98495	0.98745	0.9948	0.0013
Flattop-25	1.002	1.00308	0.99837	0.99821	1	0.003
Jezebel	0.99913	0.9998	0.99746	0.99865	1	0.002
Jezebel-240	1.00018	0.99976	1.00148	0.99849	1	0.002
Flattop-Pu	0.99684	1.00105	0.99208	0.9991	1	0.003
THOR	1.00173	0.99824	1.00743	0.99792	1	6.00E-04
Jezebel-233	0.99885	0.99975	1.00415	0.99917	1	0.001
Flattop-23	0.99855	0.99918	0.99835	0.99819	1	0.0014

Table 2-3 Results of ORNL series assemblies

Assembly	CENDL-3.1	ENDF/B-VII.0	JENDL-3.3	JENDL-4.0	Experiment	Error
ORNL-10	1.00047	0.99941	0.99928	0.99871	1.0015	0.0026
ORNL-1	1.00103	0.99878	0.99981	0.99889	1.0012	0.0026
ORNL-2	0.99981	0.9977	0.99881	0.99805	1.0007	0.0036
ORNL-3	0.99627	0.99399	0.99487	0.99435	1.0009	0.0036
ORNL-4	0.99799	0.99587	0.99666	0.99595	1.0003	0.0036



Table 2-4 Results of PNL solution assemblies

Assembly	CENDL-3.1	ENDF/B-VII.0	JENDL-3.3	JENDL-4.0	Experiment	Error
PNL-1	1.01198	1.00569	1.00859	1.00749	1	0.0032
PNL-2	1.00612	1.0001	1.00376	1.00253	1	0.0065
PNL-3	1.00752	1.00562	1.00923	1.00641	1	0.0034
PNL-4	1.00527	1.00372	1.00547	1.00271	1	0.0031
PNL-5	1.00724	1.00081	1.0047	1.00334	0.9969	0.0038
PNL-6	1.00737	1.00156	1.00512	1.00314	1	0.0065
PNL-7	1.00925	1.00361	1.00689	1.005	1	0.0047
PNL-8	1.0108	1.00481	1.00821	1.00616	1	0.0032
PNL-12	1.00876	1.00368	1.00632	1.00529	1	0.0025

Table 2-5 Results of PNL MOX fuel assemblies

Assembly	CENDL-3.1	ENDF/B-VII.0	JENDL-3.3	JENDL-4.0	Experiment	Error
PNL-30	0.99699	1.00014	0.99613	0.99963	1.0024	0.006
PNL-31	1.00166	1.00051	1.00043	1.00292	1.0009	0.0047
PNL-32	1.00235	1.00088	1.00051	1.00217	1.0042	0.0031
PNL-33	1.00588	1.00708	1.00749	1.01016	1.0024	0.0024
PNL-34	1.00363	1.0032	1.00488	1.00412	1.0038	0.0025
PNL-35	1.00864	1.00761	1.00846	1.00785	1.0029	0.0027



## ***Fast Criticality Benchmark Testing for $^{233}\text{U}$***

The evaluations for  $^{233}\text{U}$  from CENDL-3.1, ENDF/B-VII.0, JENDL-3.3 and JENDL-4.0 were tested with six U233-Metal-Fast benchmarks from ICSBEP Handbook. Total 10 criticality cases with core spectra change from hard to soft one by one, including one bare highly enriched  $^{233}\text{U}$  core and 9 cores reflected with HEU, NU, Be and W separately. The criticality calculations were performed with Monte Carlo code MCNP4C. The ACE libraries used in the calculations were prepared with NJOY99.

The C/E values of  $k_{\text{eff}}$  for selected benchmarks calculated based on CENDL-3.1, ENDF/B-VII.0, JENDL-3.3 and 4.0 are listed in Table 6 and plotted against energy spectrum index EALF, which can be used to represent the “hard” or “soft” of the core spectrum. When the EALF gets smaller and smaller in Fig.2-4, which means the spectrum of the cores gets softer and softer, the C/E values calculated with CENDL-3.1 were underestimated more and more obviously. The most under prediction is about 1200 pcm for UMF005\_2. The trend of C/E values shows seriously spectrum bias. Though spectrum trend in results of ENDF/B-VII.0 and JENDL-4.0 are not certain, under prediction of C/E values for 3 cases still found.





Table 2-6 Comparison of C/E value of  $k_{\text{eff}}$

Case ID	EALF (MeV)	$k_{\text{eff,exp}}$	uncertainty	C/E value of $k_{\text{eff}}$				Reflector
				ENDF/B-VII.0	CENDL-3.1	JENDL-3.3	JENDL-4.0	
UMF001_1	1.120	1.0000	0.0010	0.9998	0.9989	1.0034	0.9992	--
UMF002_1	1.080	1.0000	0.0010	0.9997	0.9970	1.0026	0.9985	HEU
UMF002_2	1.050	1.0000	0.0011	0.9985	0.9981	1.0035	0.9998	HEU
UMF003_1	1.080	1.0000	0.0010	0.9998	0.9983	1.0038	0.9992	NU
UMF003_2	1.070	1.0000	0.0010	0.9992	0.9984	1.0044	0.9993	NU
UMF004_1	0.999	1.0000	0.0007	1.0053	0.9941	1.0019	0.9998	W
UMF004_2	0.916	1.0000	0.0008	1.0061	0.9902	0.9987	0.9975	W
UMF005_1	0.936	1.0000	0.0030	0.9975	0.9906	0.9971	0.9961	Be
UMF005_2	0.749	1.0000	0.0030	0.9961	0.9880	0.9958	0.9957	Be
UMF006_1	1.020	0.9992	0.0014	0.9931	0.9993	1.0043	0.9990	NU



Further, analysis has been done with the reference-group method. The benchmarks used above are identified as test-group. Highly enriched uranium and plutonium cores reflected with Be, case HMF009\_1, HMF058\_4, HMF058\_5, PMF019\_1 and PMF018\_1, are introduced and served as reference-group, which have similar EALF values. The C/E values for reference-group were also calculated with CENDL-3.1 library. Fig.2-5 shows the comparison of reference-group and test-group. Since no similar  $k_{\text{eff}}$  trend against EALF can be found in reference group, the influence of the evaluation for reflector materials are excluded. And the under prediction trend relay on EALF caused by  $^{233}\text{U}$  evaluation can be identified.

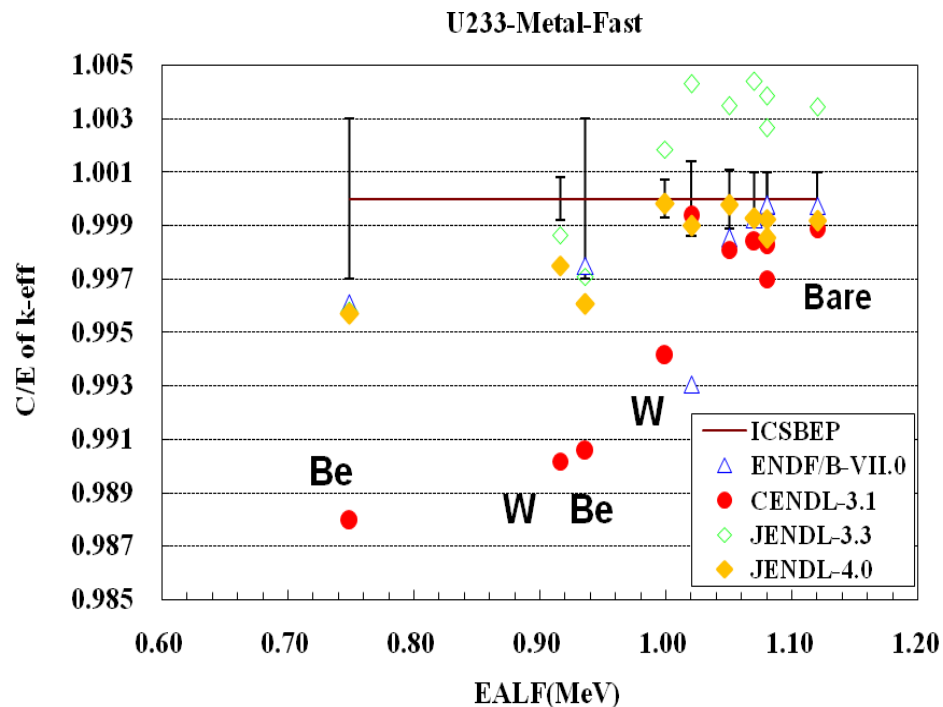


Fig.2-4 Comparison of C/E values of  $k_{\text{eff}}$  for UMF benchmarks

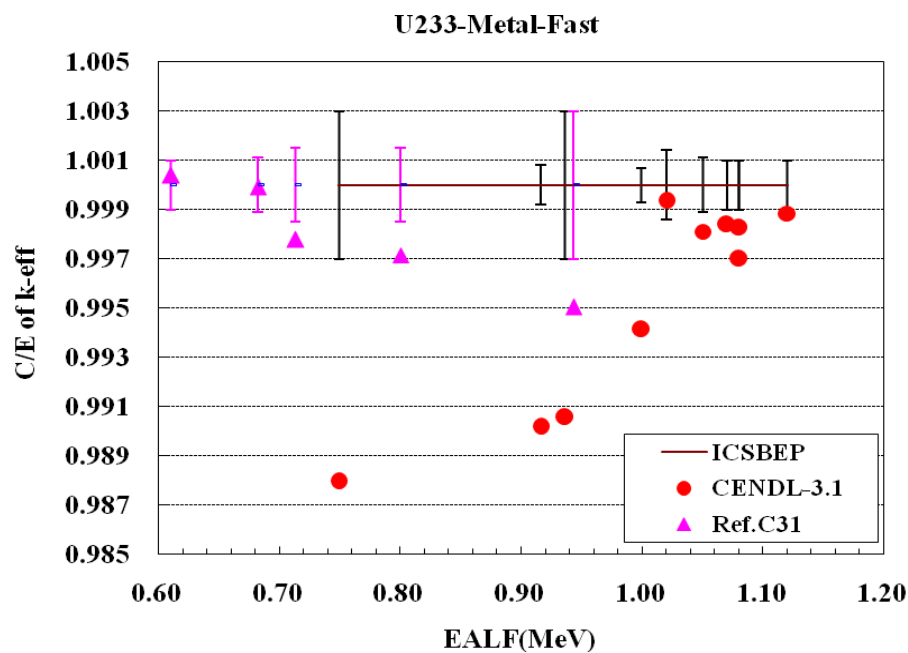


Fig.2-5 Comparison of C/E values of  $k_{\text{eff}}$  for test-group and reference-group



## ***CENDL-3.1 Data Testing with LLNL Pulsed Sphere Benchmarks***

Lawrence Livermore pulsed sphere experiments were modeled using Monte Carlo N-Particle Code (MCNP) for the purpose of benchmarking the new release of CENDL-3. This program consisted of 96 different experiments on 28 different spheres, including:  $^6\text{Li}$ ,  $^7\text{Li}$ , Be, C, N, O, Al, Mg, Ti, Fe, Cu, Ta, Au, W, Pb, Nb, Sn,  $^{232}\text{Th}$ ,  $^{235}\text{U}$ ,  $^{238}\text{U}$ ,  $^{239}\text{Pu}$ , LiD, Air,  $\text{H}_2\text{O}$ ,  $\text{D}_2\text{O}$ , polythene, teflon and concrete. The calculated results were compared to experimental results, the results obtained from CENDL-2.1, ENDF/B-VII, JENDL-3.3 and JEFF-3.1 (as shown in Fig.2-6).

Through the analysis for the microscopic cross section and double differential spectrum of those nuclides with microscopic experimental data, further conclusions and suggestions can be obtained.

The results show that the results of new release CENDL-3.1 give better results in comparison to experiment to CENDL-2.1, and close to other libraries. The light nuclei results are match the experiment well. And the results of Cu, Fe, Mg of CENDL-3.1 give better results in comparison to experiment to ENDF/B-VII. But the F, N, Ti,  $^{239}\text{Pu}$ , Ta, Au, W, Nb of CENDL-3.1 results give deviation results in comparison to experiment to other libraries, the evaluated nuclear data were proposed further improvements.



LLNL Pulsed Sphere, Mg, 0.7 mfp, Pilot B 1.6MeV bias, 765.2cm

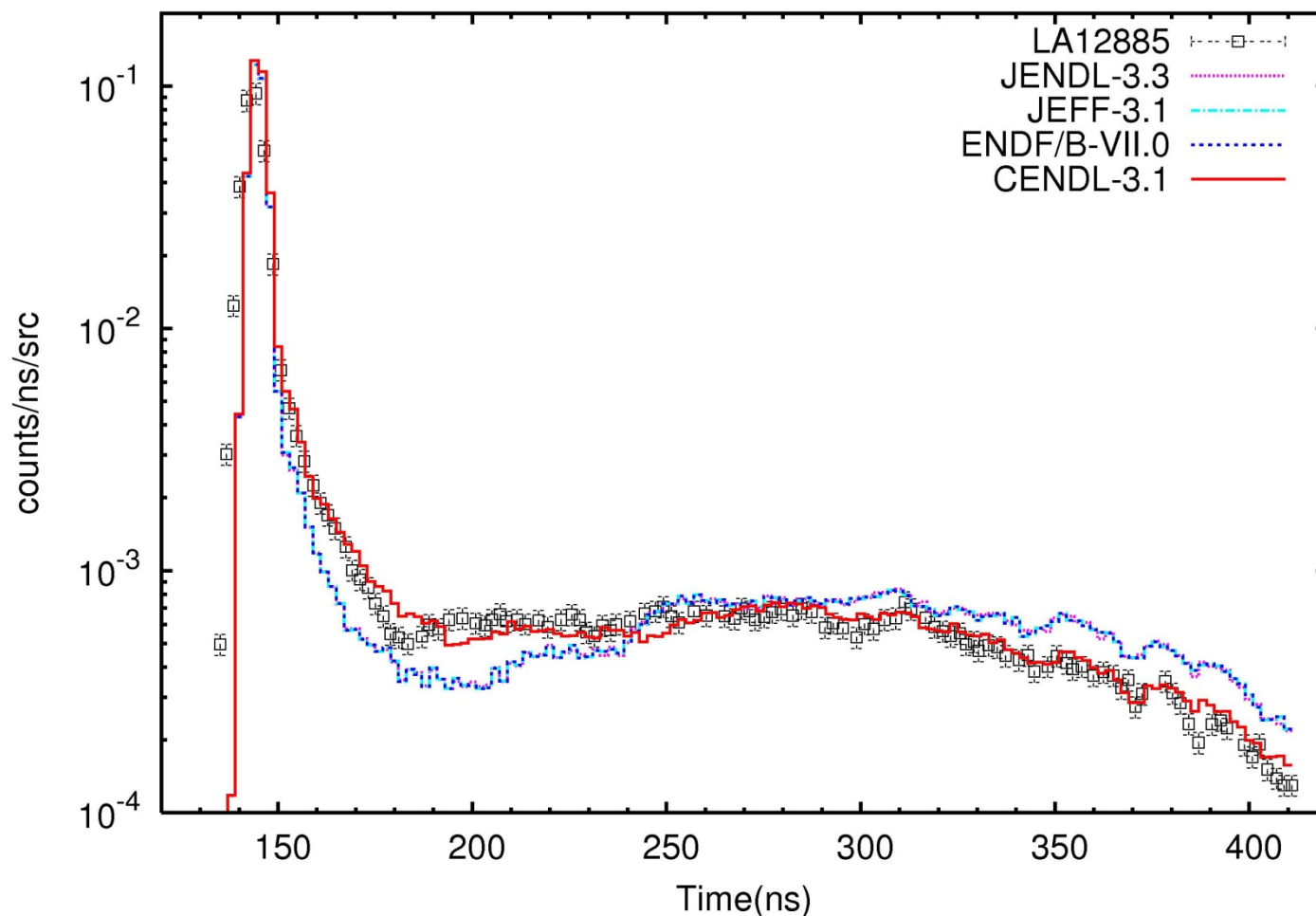


Fig.2-6 Neutron spectrum for the LLNL Pulsed Sphere, Mg (0.7 mfp) benchmark



## 2.3 Methodology Studies

### *The Status of Covariance Evaluation at CNDC*

To determine the uncertainty of neutron cross sections for modern nuclear data application, the covariance evaluation system, COVAC, is being developed at CNDC to achieve the covariance files **mainly for structure and fission nuclides** in CENDL. In this system, experimental data including their errors were firstly pre-analyzed and handled via some available tools. It is worth mentioning that different approaches were developed to deal with the data and errors from different experimental techniques, such as activation method and TOF;

At the same time, the various reaction data were also treated in different way. Secondly, one subsystem-SEMAW, was specially designed to calculate sensitive matrices of various theoretical model parameters for different nuclear reaction codes (the UNF code series, DWUCK and ECIS are currently incorporated in SEMAW). In this framework, the high fidelity covariance file can be obtained with combining the theoretical and experimental uncertainties and correlations. So far, our methodology can be suitable to the fast neutron range, and the resonance energy region is under discussion.

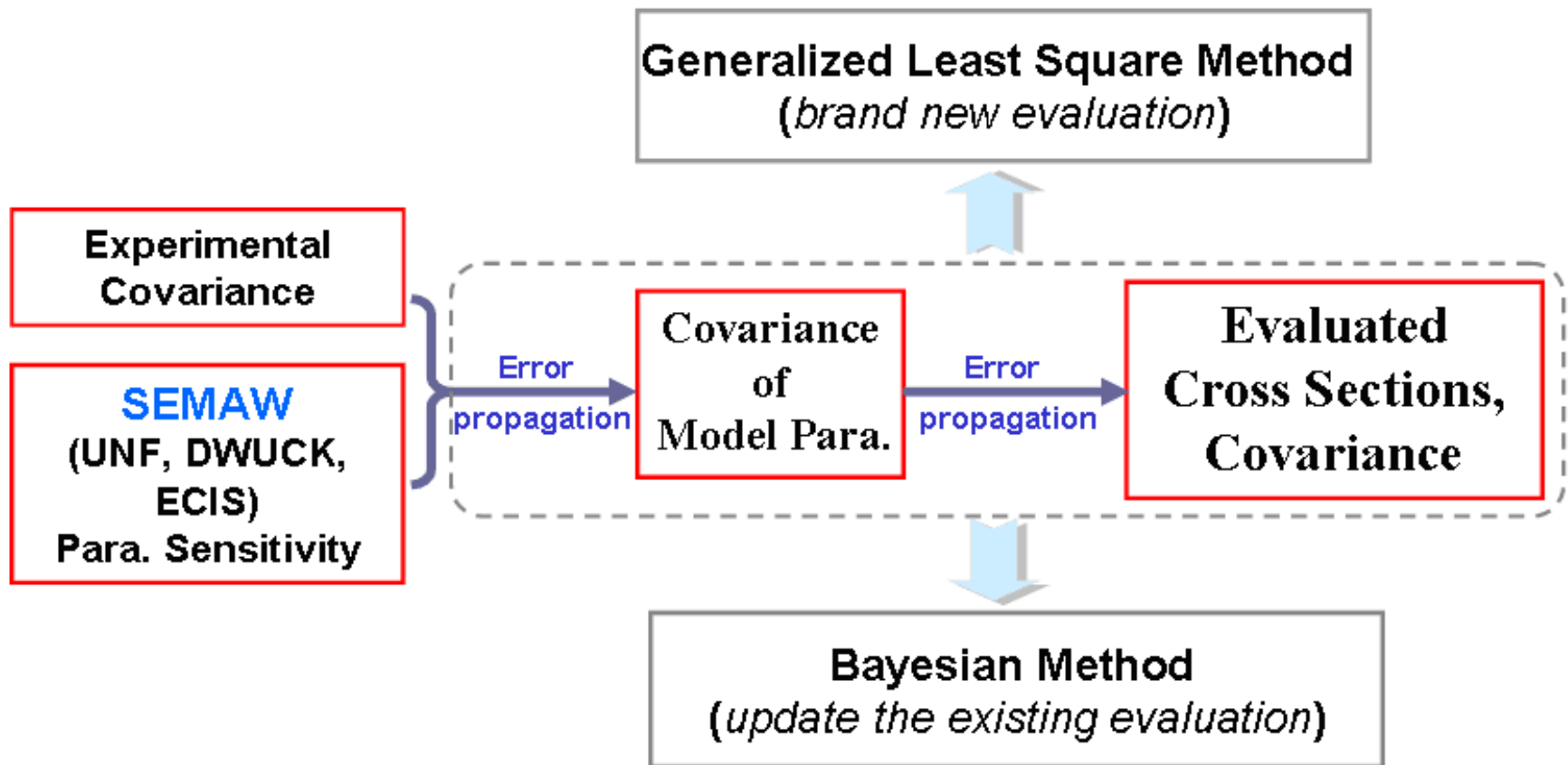


Fig. 2-7 COVAC SYSTEM OF CNDC



Recently, more concentration in CNDC were paid on evaluating the experimental covariance information, collecting the experimental techniques and their characters, at the same time, we are making effort to build a new assistant evaluation software to make the process easier. Here,  $^{40}\text{Ca}(n, a)$  is sampled to explain the procedure.

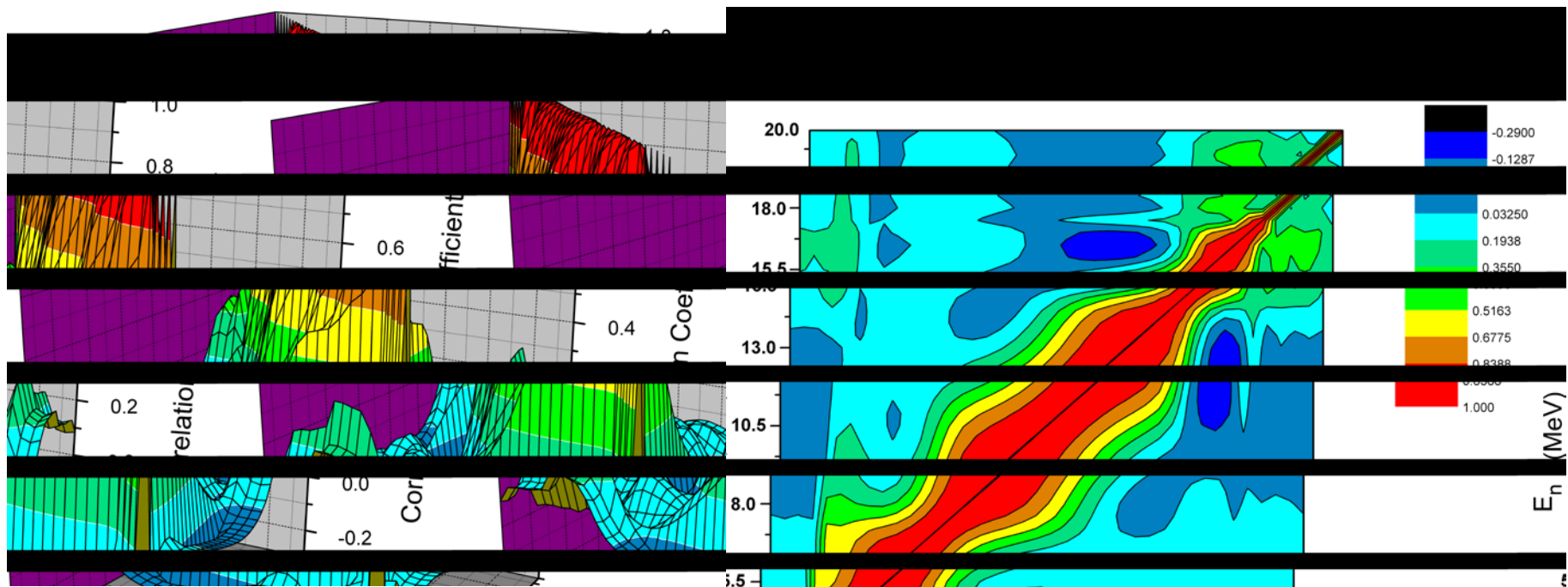


Fig.2-8 The correlation coefficient matrix of the  $^{40}\text{Ca}(n, a)$  fit cross sections





## ***Semi-Empirical Study on the Yield Energy Dependence of the $^{235}\text{U}+n$ Fission***

A semi-empirical model based upon the basic idea of Multi-Modal Random Neck-Rupture Model was applied to study the yield energy dependence of  $^{235}\text{U}+n$  fission. The compound system energy was simplified including the macro energy and shell effects. The 11 parameters in the model were determined by fitting the evaluated experimental data. The fragment level density was determined by taking into account of the compound and fragment characters, which could improve the results. The shell effect weakened with temperature was illustrated. Prompt fission neutron and multichannel fissions were also taken into account.

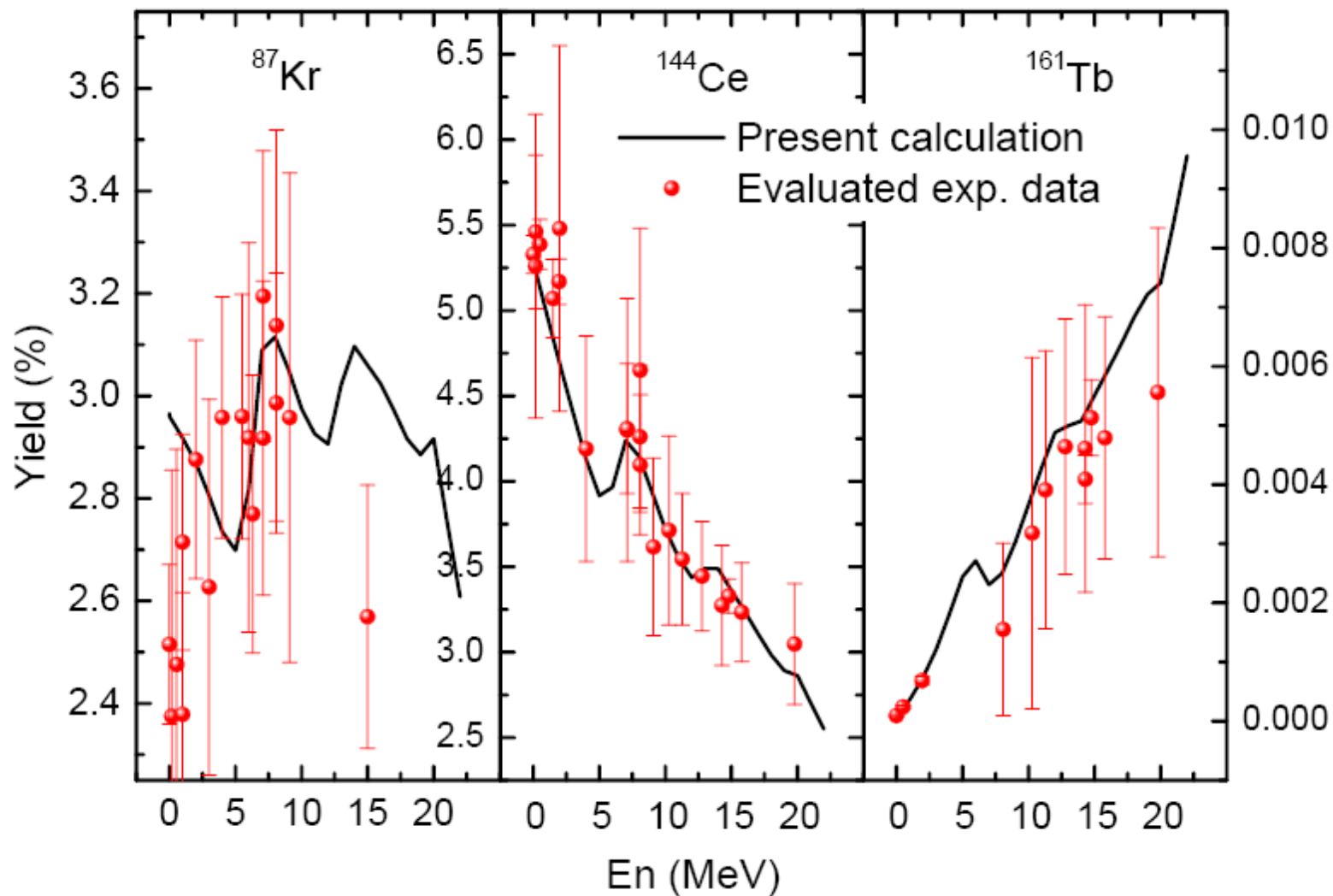


Fig.2-9 Yield energy-dependence of  $^{87}\text{Kr}$ ,  $^{144}\text{Ce}$ ,  $^{161}\text{Tb}$  of  $^{235}\text{U}+n$  fission

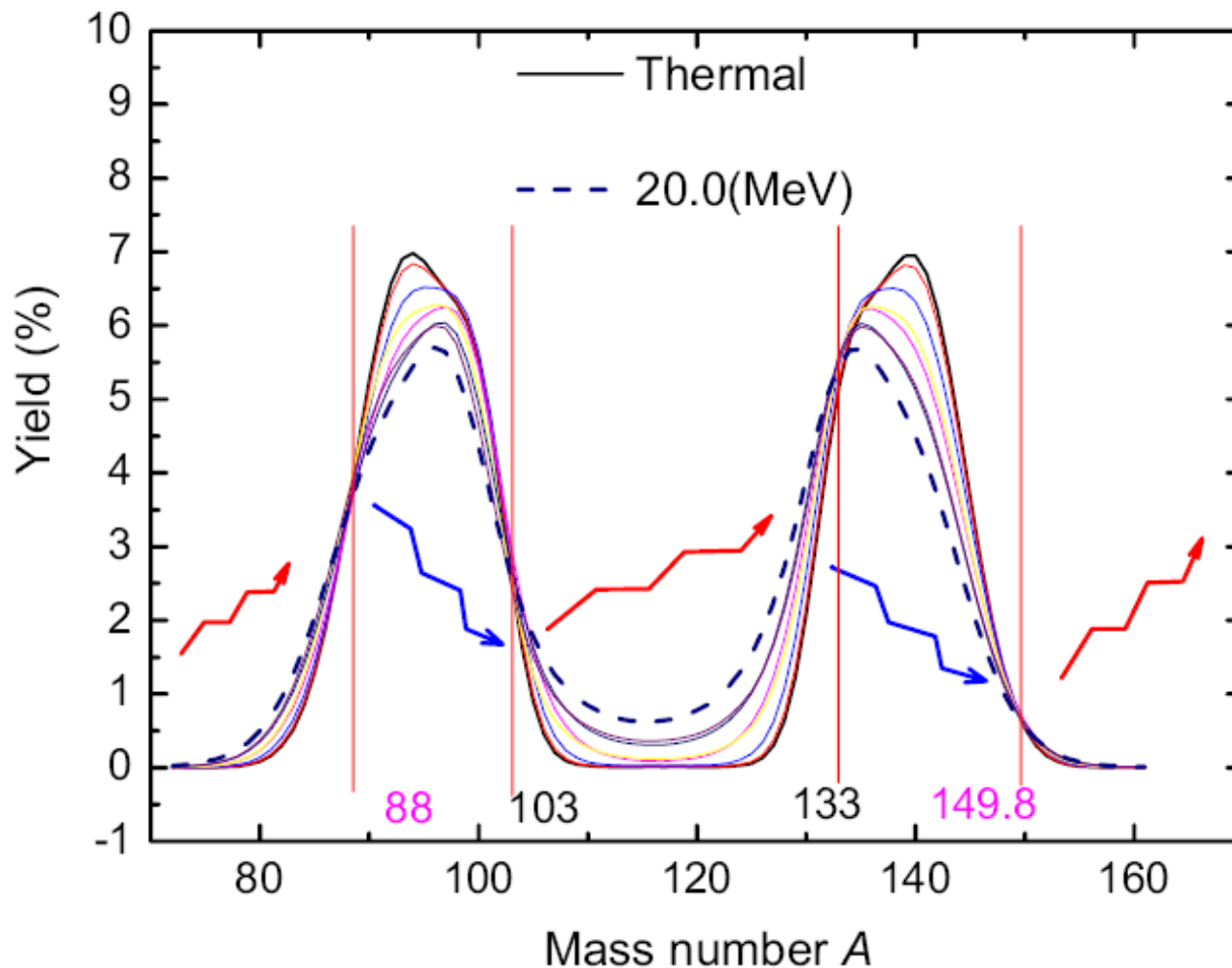


Fig.2-10 Mass distributions of the  $^{235}\text{U}+n$  fission. 5 mass distribution curves from energies 0.5 MeV to 18 MeV are shown in addition to the thermal and 20 MeV curves. The arrows indicate the yields step-increased or -decreased with the energy.



The mass distribution of fission fragments can be reproduced well by the model. The yield dependence on energy of part fragments and the shapes of most of the fragments can be described by the model. The results show that the yield step-increased with the energy over the fragment masses at wings and valley, step-decreased over peaks, and vibrated near the joints ( $A=88$ , 103, 133 and 149.8). The 'step' is believed to be arose by the opening of the multi-channel fission. The yield ratio of SL fission to the total, as well as the standard I to the total, increased with the energy, while Standard II decreased. It is shown by model study that there exist systematic disagreement among the experimental data measured with radioactive and kinetic different methods, which made more uncertainty in determination of the parameters. So fine corrections of the experimental data and improved experiment are needed.



## ***Prompt Neutron Multiplicity Distribution for $^{235}\text{U}(n,f)$ at Incident Energies Up to 20 MeV***

The total excitation energy partitions between the complementary light and heavy fission fragments for the  $n+^{235}\text{U}$  fission reaction are given at incident energies up to 20 MeV. The average neutron kinetic energy  $\langle \epsilon \rangle(A)$  and the total average energies removed by  $\gamma$  rays  $E_\gamma(A)$  as a function of fission fragment (FF) mass at different incident neutron energies are presented. The prompt neutron multiplicity distribution  $\nu(A)$  for  $n+^{235}\text{U}$  fission at different incident neutron energies are calculated. The results are checked with the total average prompt neutron multiplicities and compared with the experimental and evaluated data. These results can be used for the prompt fission neutron multiplicity and spectrum evaluation, and the calculated  $\nu(A)$  distribution provides the data to deduce the post-neutron emission mass yields from the already known pre-neutron emission mass yields. The former is very important for the application.

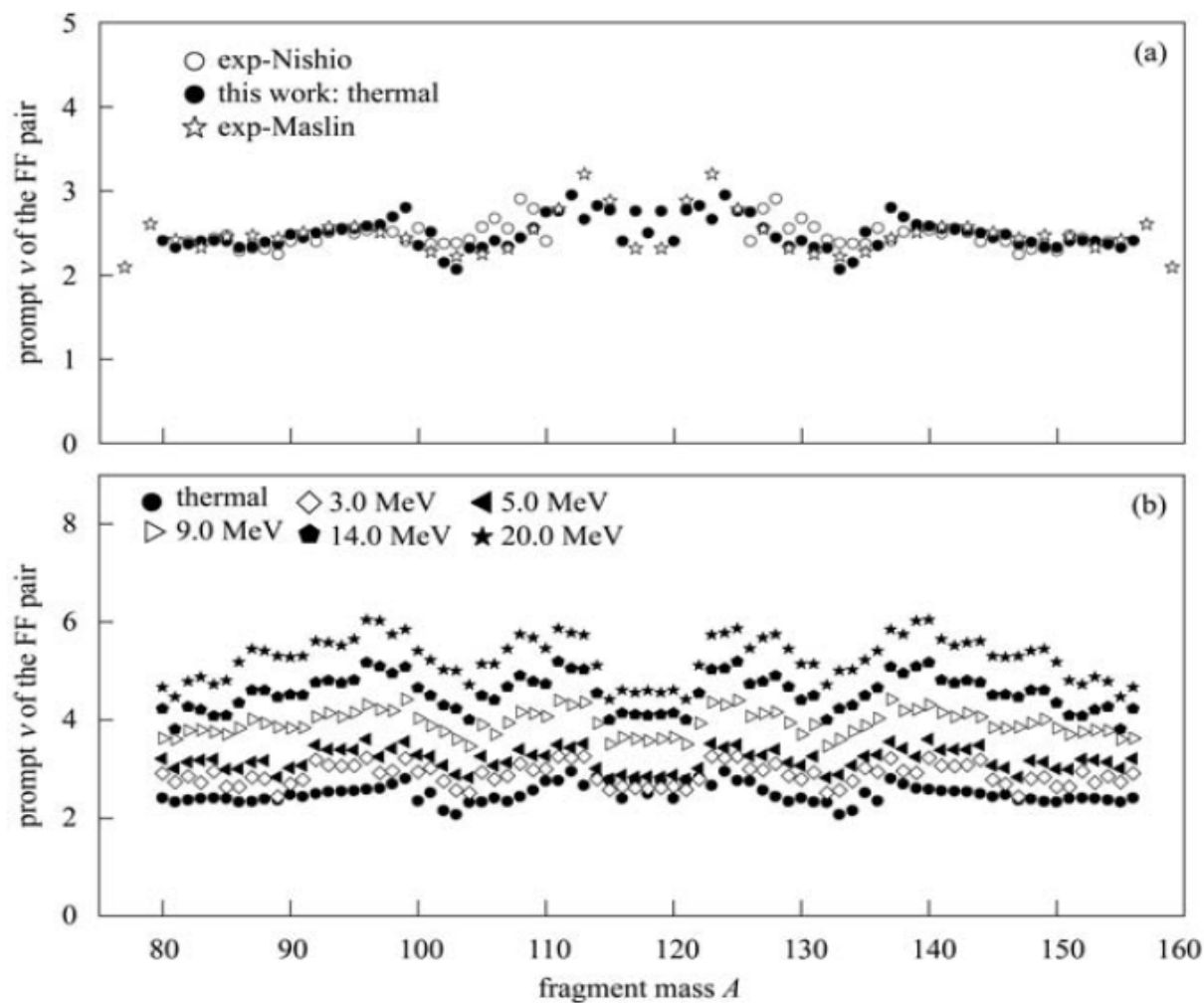


Fig. 2-11 FF pair multiplicity of the  $^{235}\text{U}(n,f)$  reaction at thermal neutron energy (a) and higher neutron energies (b)



## ***The Systematics of (n,2n) Reaction Excitation Function***

Based on the constant temperature evaporation model taking the competition of (n,3n) reaction and the contribution of pre-equilibrium emission into account, the systematics formulae of (n,2n) reaction excitation function have been established. The systematics behaviours of (n,2n) reaction excitation function have been studied. There are two systematics parameters  $T$  and  $\sigma_{n,M}$  can be adjusted in the formulae. For getting the two parameters, the new evaluated data of (n,2n) reactions were adopted and fitted by means of the nonlinear least squares method. The fitted results agree fairly well with the measured data at  $45 \leq A \leq 210$  below 30 MeV. Based on a body of new measurements, the reliability to predict (n,2n) reaction excitation function is improved. Hence more accurate systematics prediction for unmeasured nucleus or energy range may be provided.

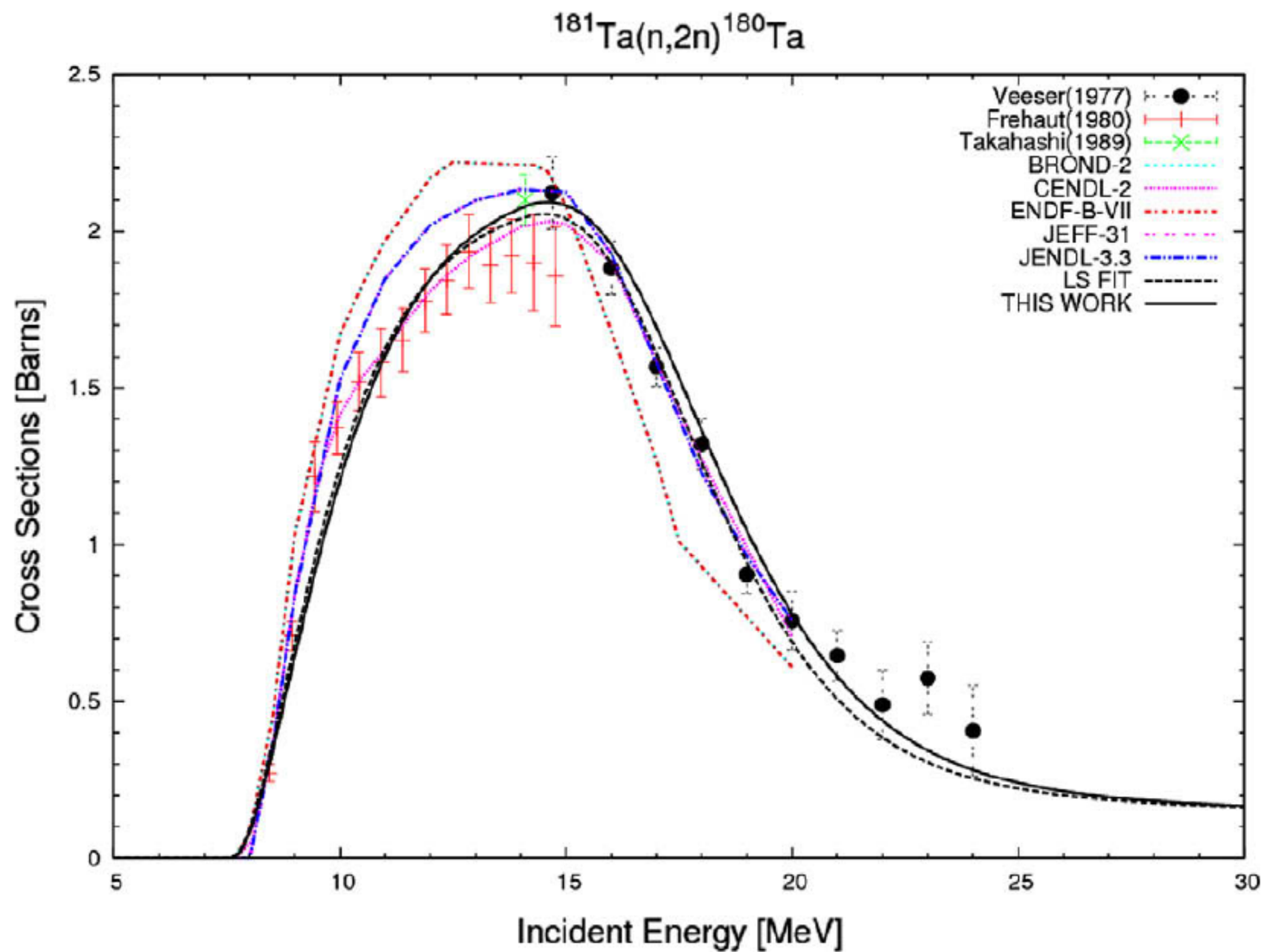


Fig.2-12 Excitation function of the (n,2n) reaction for  $^{181}\text{Ta}$





## 2.4 EXFOR Compilation at CNDC

A group (3 staff from evaluation unit, 1 from data library unit of CNDC) to do the EXFOR database compilation.

There are charged for compilation of EXFOR for the journals published in China and some other articles made by Chinese published outside of Chinese journals.

The list of Chinese journals related to nuclear data measurement

Name and Code of Journal	History of Journal
<b>Journal of High Energy Physics and Nuclear Physics (HEN/PHE)</b> (高能物理与核物理)	<b>1997 established (Chinese)</b> <b>2007 Chinese Physics C (English)</b> (中国物理)
<b>Atomic Energy Science and Technology(CST)</b> (原子能科学技术)	<b>1959 established (Chinese)</b>
<b>Journal of Nuclear and Radiochemistry (HFH)</b> (核化学与放射化学)	<b>1979 established (Chinese)</b>
<b>Nuclear Physics Review</b> (原子核物理评论)	<b>1984 established (Chinese)</b>
<b>Nuclear Technology(CNST)</b> (核技术)	<b>1978 established (Chinese)</b> <b>1989 Nuclear Science and Techniques (English)</b> (核技术)
<b>Chinese Physics Letters (CPL)</b> (中国物理快报)	<b>1989 established (English)</b>



## **3. Activities of Nuclear Data Measurement**

### ***3.1 The Facilities Used for the Nuclear Data Measurements and Study***

#### **Peking University:**

4.5-MV Van de Graaff accelerator

#### **Lanzhou University:**

300kV -Cockcroft-Walton accelerator (neutron flux:  $8 \times 10^{12} \text{n/cm}^2 \cdot \text{s}$ )

#### **China Institute of Atomic Energy:**

HI-13 tandem accelerator,

600kV-Cockcroft-Walton accelerator, (neutron flux:  $8 \times 10^{11} \text{n/cm}^2 \cdot \text{s}$ )

5SDH-2 tandem accelerator,

China Advanced Research Reactor. (CARR, neutron flux:  $8 \times 10^{14} \text{n/cm}^2 \cdot \text{s}$ )

China Experimental Fast Reactor (CEFR, 65 MW)

... et al.



## *The China Advanced Research Reactor.*

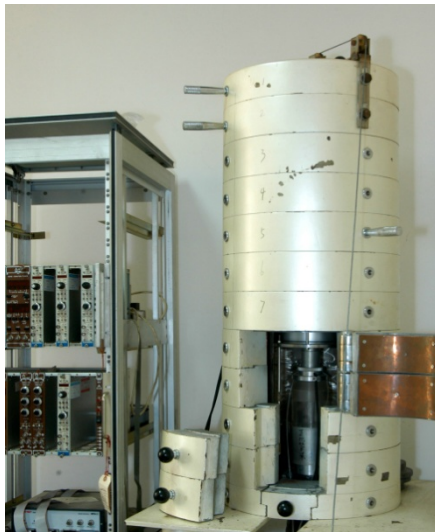




## ***The China Experimental Fast Reactor.***









## ***China Spallation Neutron Source(under construction)***

China Spallation Neutron Source (CSNS) is a large scientific facility dedicated chiefly to multidisciplinary research on material characterization using the neutron scattering techniques.

This project was officially approved by the Chinese central government in 2008, and will be built in phases with the first phase (CSNS-I) to produce protons of 100 kW in beam power. The CSNS accelerator is designed to deliver proton beam with an energy of 1.6 GeV and a pulse repetition rate of 25 Hz to a tungsten target (TS1). At TS1, it is planned to build 18 neutron beam lines for neutron scattering.

The back-streaming neutrons that are modestly moderated by the cooling water passing through the target slices have a very wide energy spectrum (the so-called white neutrons), and are very suitable for nuclear data measurements.

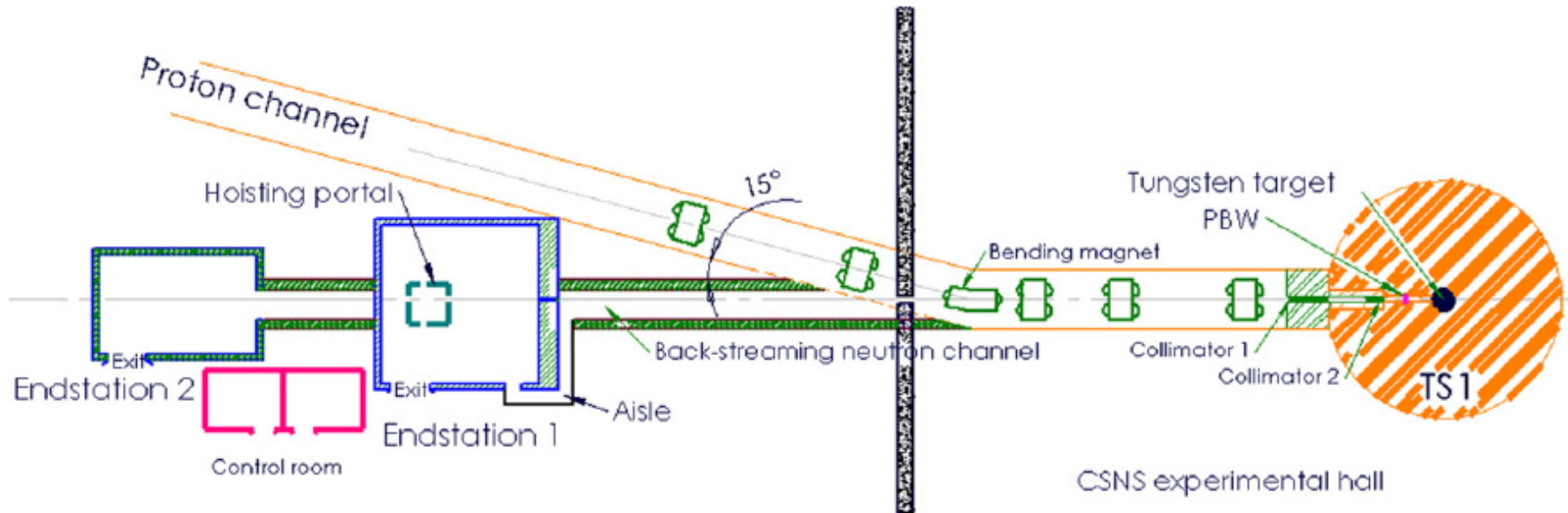


Fig. 3-1. Schematic layout of the back-streaming neutron endstation



The main characteristics of the neutron beam based on the simulations by FLUKA are summarized in following table.

Table 3-1 The main characteristics of the neutron beam  
on the back-streaming neutron endstation.

Neutron energy range	1eV-1 MeV
Proton beam energy and intensity	1.6 GeV and $1.6 \times 10^{13}$ (p/pulse)
Pulse repetition rate	25 Hz
Neutron flux at 80 m(uncollimated)	$2.0 \times 10^5$ n/cm <sup>2</sup> /pulse
Fraction of flux in 1eV-1MeV range (uncollimated)	0.53





## ***3.2. Nuclear Data Measurements and Related Activities***

In recent years, A lot of neutron cross section, angular distribution, neutron emission spectra, double differential cross section and nuclear decay data for a mount of nuclei have been measured and the results have been evaluated and provide to the users. Many method studies of the nuclear data measurements were performed and some study fruits of them have been used in our nuclear data measurements.

### ***Decay Data Measurement and Evaluation***

In recent years, the decay data for  $^{56}\text{Co}$ ,  $^{66}\text{Ga}$ ,  $^{213}\text{Bi}$ ,  $^{213}\text{Po}$ ,  $^{217}\text{At}$ ,  $^{217}\text{Rn}$ ,  $^{221}\text{Fr}$ ,  $^{223}\text{Fr}$ ,  $^{225}\text{Ac}$ ,  $^{225}\text{Ra}$ ,  $^{231}\text{Th}$ ,  $^{234,234\text{m}}\text{Pa}$ ,  $^{235}\text{U}$  nuclides have been updated and recommended using available experimental data. The recommended data and evaluated comments were published in DDEP website.

Also China group has re-evaluated the main relative  $\gamma$ -ray intensities for  $^{56}\text{Co}$  and  $^{66}\text{Ga}$  considered China measurements for high energy calibration of Ge detectors. The results are listed in Table 3-2 and Table 3-3.



Table 3-2 Main measured and evaluated relative  $\gamma$ -ray intensities for  $^{56}\text{Co}$

$E_\gamma$	Measurements				Evaluations	
(keV)	Raman(2000)	Molnar(2002)	Y.Weixiang(2006)	Dryak(2008)	IAEA(Rec.)	Present(Rec.)
846.8	100.0	100.0(2)	100.0(5)	100	100	100.0
1037.8	14.11(22)	14.07(5)	14.15(8)	14.10(6)	14.04(5)	14.09(3)
1175.1	2.25(4)	2.252(10)	2.26(2)	2.258(7)	2.250(9)	2.253(6)
1238.3	66.6(10)	66.20(17)	66.26(26)	66.68(20)	66.45(16)	66.27(18)
1360.2	4.23(7)	4.22(15)	4.26(3)	4.32(4)	4.283(13)	4.273(3)
1771.4	15.42(25)	15.24(8)	15.36(9)	15.39(8)	15.46(4)	15.45(3)
2015.2	3.03(5)	2.976(15)	3.02(2)	3.018(24)	3.019(14)	3.019(8)
2034.8	7.835(120)	7.69(3)	7.79(5)	7.814(40)	7.746(13)	7.758(17)
2598.5	17.1(3)	16.82(8)	16.62(12)	17.03(15)	16.97(4)	16.76(12)
3202.0	3.16(6)	3.196(18)	3.16(3)	3.243(30)	3.205(13)	3.134(13)
3253.4	7.815(160)	7.85(4)	7.62(6)	7.99(2)	7.87(3)	7.66(3)
3273.0	1.84(4)	1.854(13)	1.82(2)	1.899(8)	1.856(9)	1.815(4)
3451.2	0.93(3)	0.94(1)	0.919(10)	0.951(10)	0.943(6)	0.926(8)



Table 3-3 Main measured and evaluated relative  $\gamma$ -ray intensities for  $^{66}\text{Ga}$

$E_\gamma$	Measurements				Evaluations	
(keV)	Raman(2000)	Molnar(2002)	Baglin(2002)	Y.Weixiang(2006)	IAEA(Rec.)	Present(Rec.)
833.6	16.02(24)	15.92(6)	15.94(14)	15.85(17)	15.93(6)	15.92(5)
1039.4	100.0(16)	100.0(3)	100.0(9)	100.0(5)	100.0(3)	100.0
1333.2	3.17(5)	3.171(13)	3.20(3)	3.15(2)	3.175(13)	3.17(1)
1918.8	5.33(8)	5.360(23)	5.44(6)	5.36(4)	5.368(23)	5.37(2)
2189.9	14.54(21)	14.39(6)	14.50(13)	14.12(12)	14.42(6)	14.37(5)
2422.9	5.12(8)	5.072(24)	5.15(6)	5.17(4)	5.085(24)	5.10(2)
2752.3	61.2(8)	61.34(26)	61.5(6)	60.80(40)	61.35(26)	60.71(6)
3229.2	4.06(8)	4.087(22)	4.07(4)	4.00(6)	4.082(22)	3.99(1)
3381.4	3.96(8)	3.950(23)	3.99(4)	3.83(4)	3.960(23)	3.86(2)
4086.5	3.38(8)	3.455(20)	3.42(4)	3.36(5)	3.445(20)	3.37(1)
4806.6	4.93(11)	5.04(3)	5.00(7)	4.99(8)	5.03(3)	4.99(3)



## ***Fission yields measurements from 0.57MeV , 1.0MeV and 1.5MeV neutrons induced fission of $^{235}\text{U}$ .***

The fission products of the fission of  $^{235}\text{U}$  induced by 0.57MeV, 1.0MeV and 1.5MeV neutrons measured at CIAE. Absolute fission rate was monitored with a double-fission chamber. Fission product activities were measured by HPGe  $\gamma$ -ray spectrometry. MCNP IVB was applied to simulate neutron spectrum in the Uranium samples, and the effects of all kinds of secondary neutrons on fission yield data were discussed.

The Fission yields of  $^{95}\text{Zr}$  we measured for 0.57MeV, 1.0MeV and 1.5MeV are 6.64%, 6.49% and 6.59%; The yield data were compared with those of other labs. The results of CIAE are in agreement with those of ANL within the scope of experimental uncertainties.

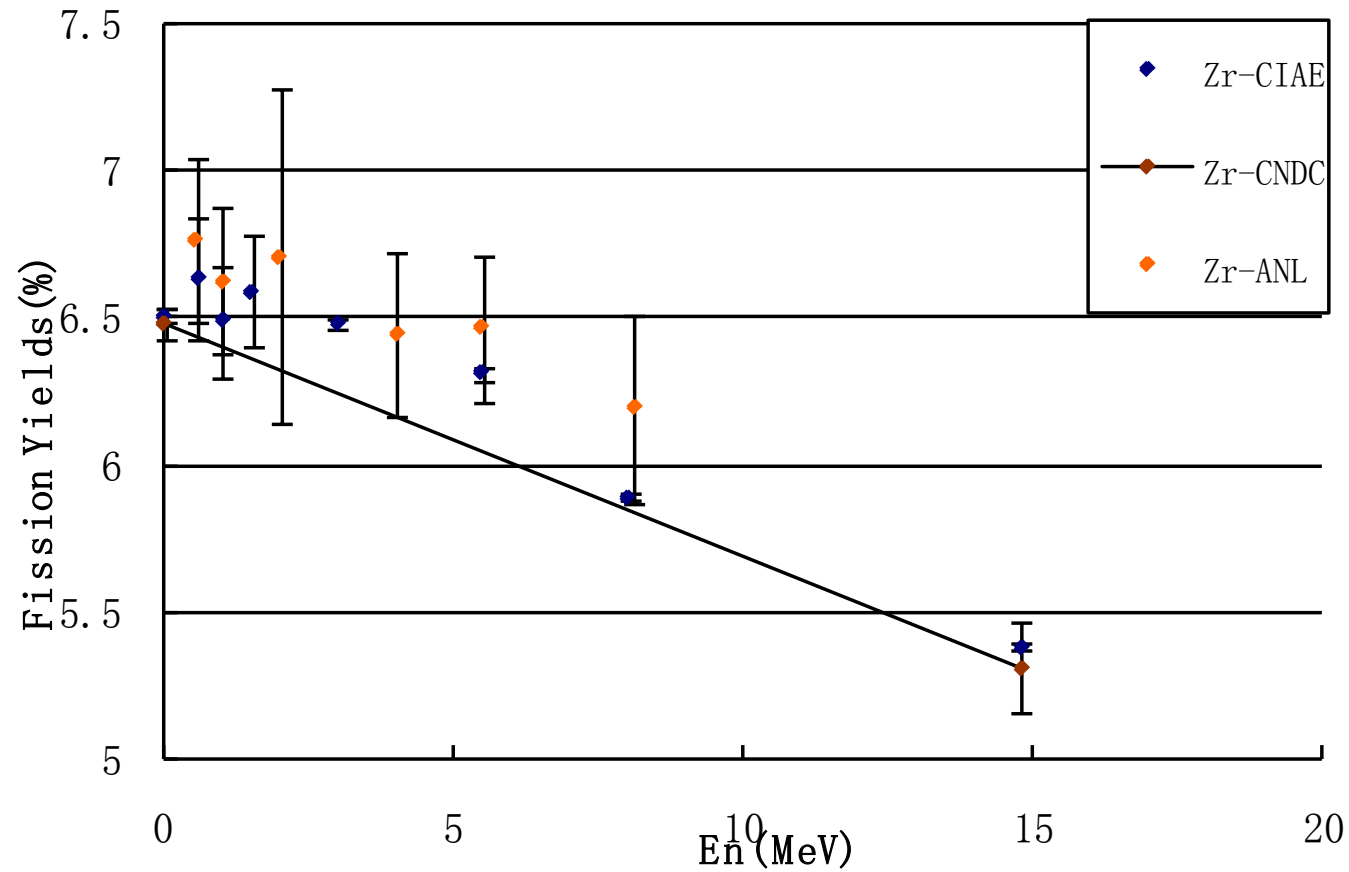


Fig 3-1. Results comparison for  $^{95}\text{Zr}$  yields



## ***Benchmarking of Evaluated Neutron Data for Uranium***

An experimental system for benchmarking of evaluated nuclear data by a 14 MeV neutron leakage spectra measurement with slab sample has been setup at CIAE.

The neutron leakage spectra from  $10 \times 10 \times 5$  cm pure uranium slab sample at 45 and 135 degrees were measured by time-of-flight technique from 15 MeV down to about 1 MeV for the first experiment.

The experimental results were compared with the calculated ones by Monte-Carlo simulation, using the evaluated data of uranium from the CENDL3.0, ENDF/B-VII and JENDL3.3 libraries. The angle dependent neutron energy spectra for the neutron source, the influence of the target material on the neutron source, the detection efficiency, the time response of the neutron detector and the width of the beam pulse were considered carefully in the simulation.

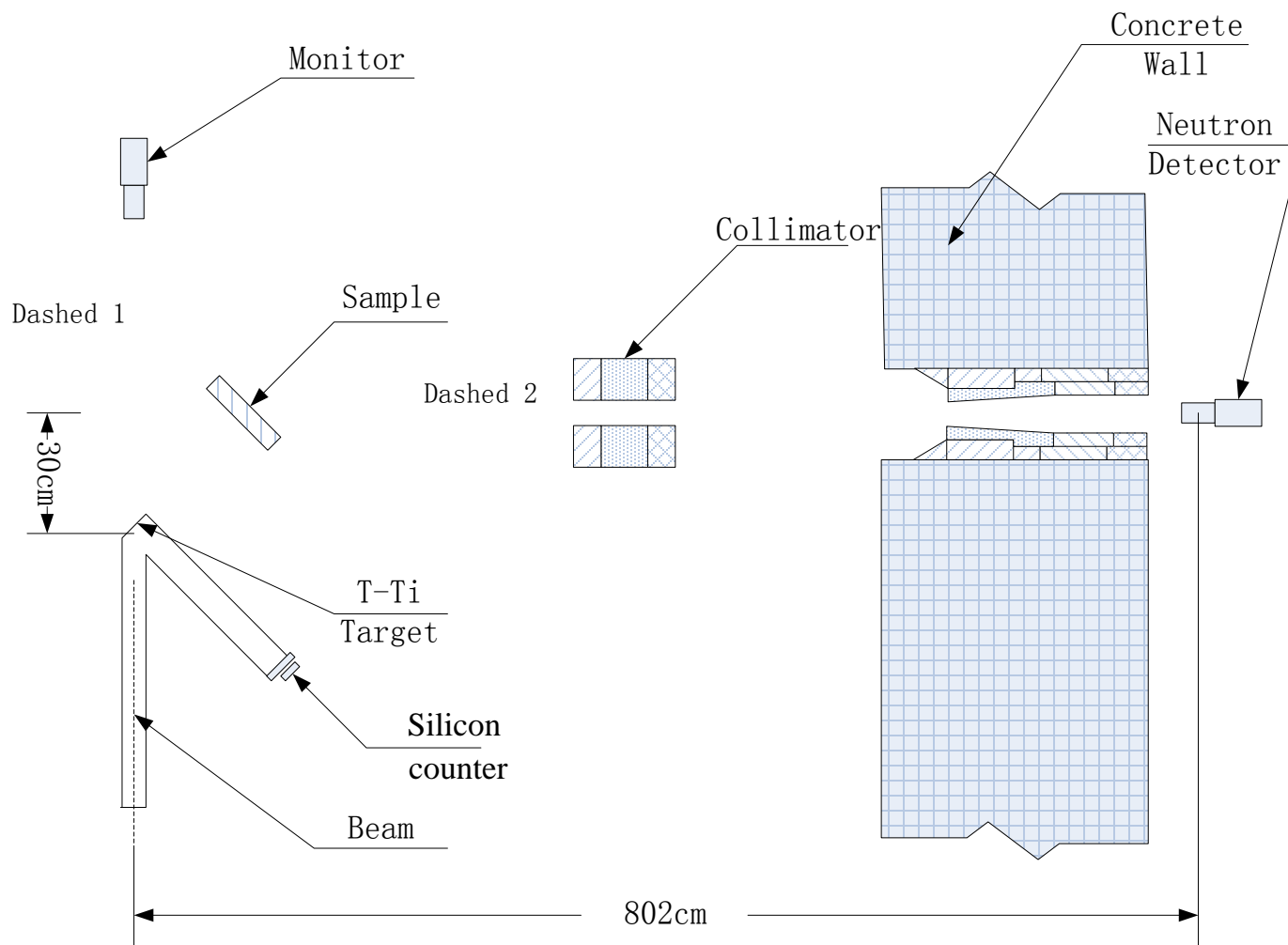


Fig.3-2 Experimental arrangement for measuring the neutron leakage spectra from uranium slab

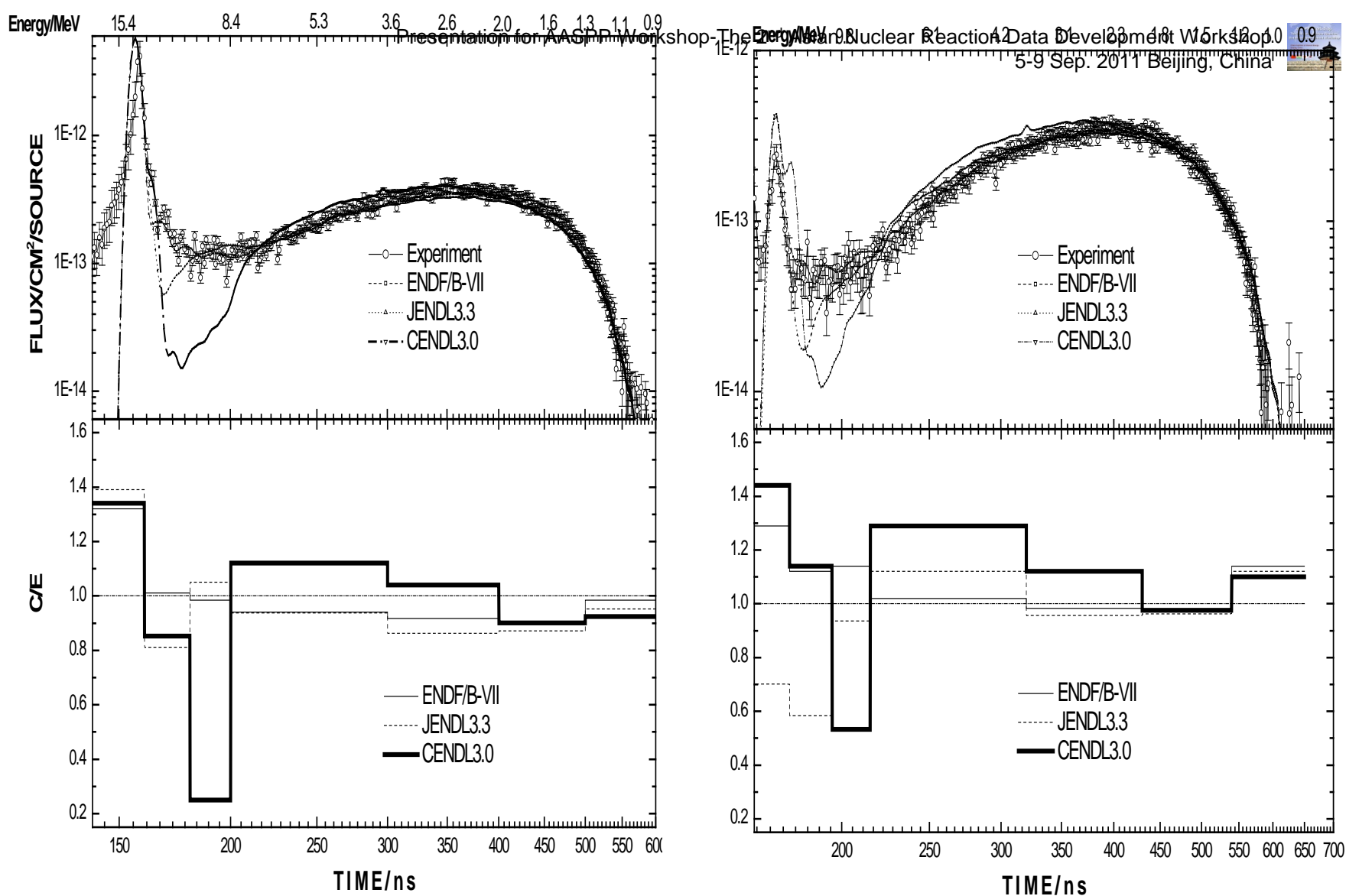


Fig.3-3 Comparison of experimental and calculated neutron leakage spectra (top) and ratio C/E (bottom) with 240 keV electron equivalent threshold.(Left: Measured at 45 degree. Right: Measured at 135 degree)





## ***Benchmarking of Evaluated Neutron Data for Large Polythene Sample***

Since Polythene (CH<sub>2</sub>)<sub>n</sub> is only composed of carbon and hydrogen nuclides, it is an ideal neutron slowing-down material. It is also a good material for verifying a neutron benchmark experiment, not only for the neutron transport code but also the experiment instrument system, by measuring the leakage spectrum of neutron transmission through a large polythene sample, because the neutron cross-sections for hydrogen and carbon are well known.

The 14.8 MeV neutrons were produced by the T(d, n)<sup>4</sup>He reaction using the 300keV D<sup>+</sup> beam accelerated by the Cockcroft-Walton accelerator, the neutron leakage spectra from the surface of the polythene slab at 20°, 30°, 40° and 50° have been measured by the time-of-flight method.

The experimental results are compared with the calculated ones by Monte-Carlo simulation. In the simulation, the angle dependent neutron energy spectra for the neutron source, the influence of the target material on the neutron source, the detection efficiency, the time response of the neutron detector and the width of the beam pulse were considered carefully. The leakage spectrum at 30° from one free-path thickness Polythene is shown in Fig.3-4. The calculated result agrees well with the experiment, this experiment gave a good verification for the benchmark experimental system.

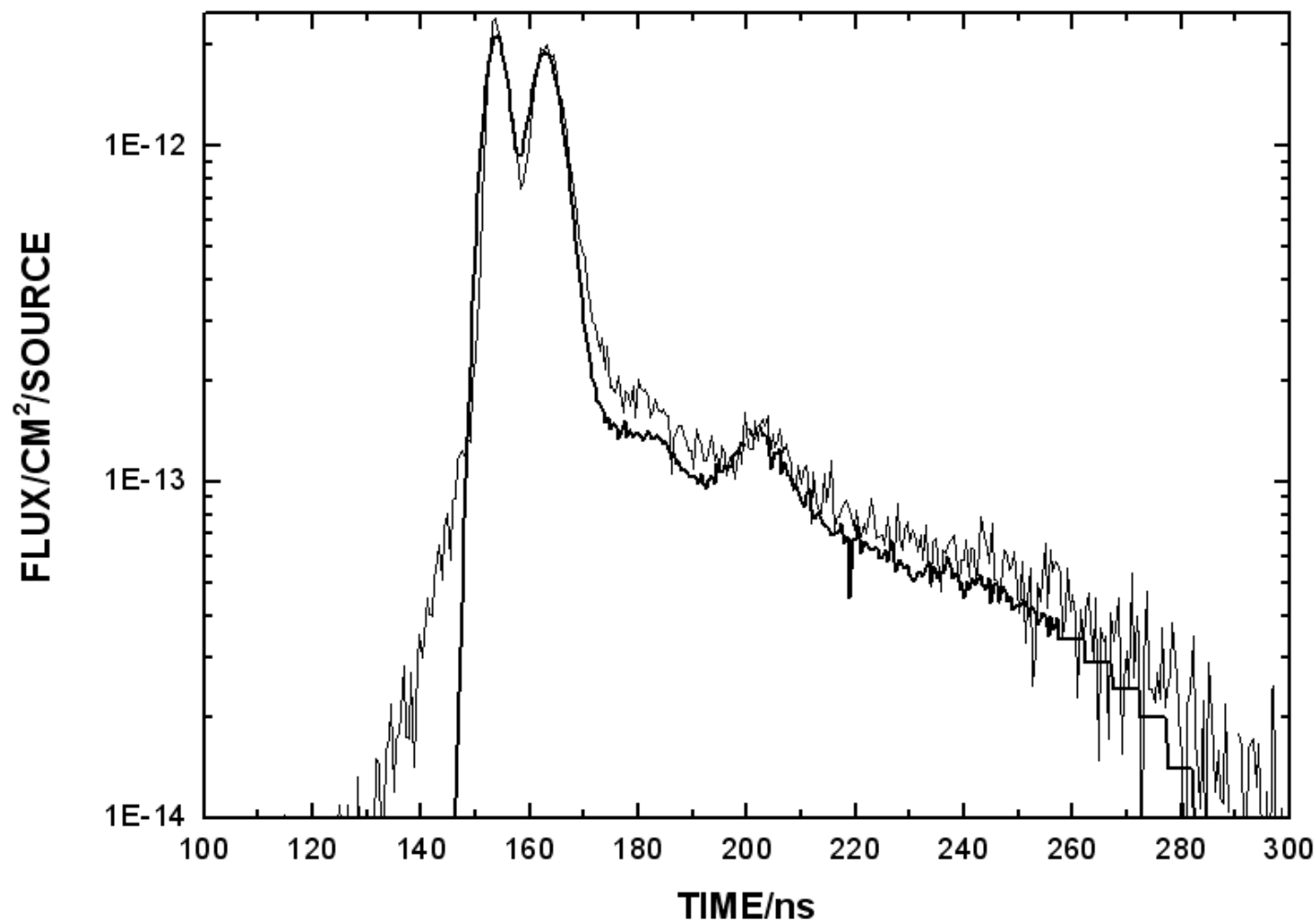


Fig.3-4 Comparison of experimental and calculated neutron leakage spectra with 240 keV electron equivalent threshold at 30°



## ***Differential cross section for neutron scattering from $^{209}\text{Bi}$ at 37 MeV and the weak particle-core coupling***

Differential scattering cross-section data have been measured at 43 angles from  $11^\circ$  to  $160^\circ$  for 37-MeV neutrons incident on  $^{209}\text{Bi}$ . The primary motivation for the measurements is to address the scarcity of neutron scattering data above 30 MeV and to improve the accuracy of optical-model predictions at medium neutron energies.

The high-statistics measurements were conducted at CIAE using the  $^3\text{H}(\text{d},\text{n})^4\text{He}$  reaction as the neutron source, a pulsed deuteron beam, and time-of-flight (TOF) techniques. Within the resolution of the TOF spectrometer, the measurements included inelastic scattering components. The sum of elastic and inelastic scattering cross sections was computed in joint optical-model and distorted-wave Born approximation calculations under the assumption of the weak particle-core coupling.

The results challenge predictions from well-established spherical optical potentials. Good agreement between data and calculations is achieved at 37 MeV provided that the balance between surface and volume absorption in a recent successful model [A.J.Koning and J.P.Delaroche, Nucl. Phys. A 713, 231 (2003)] is modified, thus suggesting the need for global optical-model improvements at medium neutron energies.

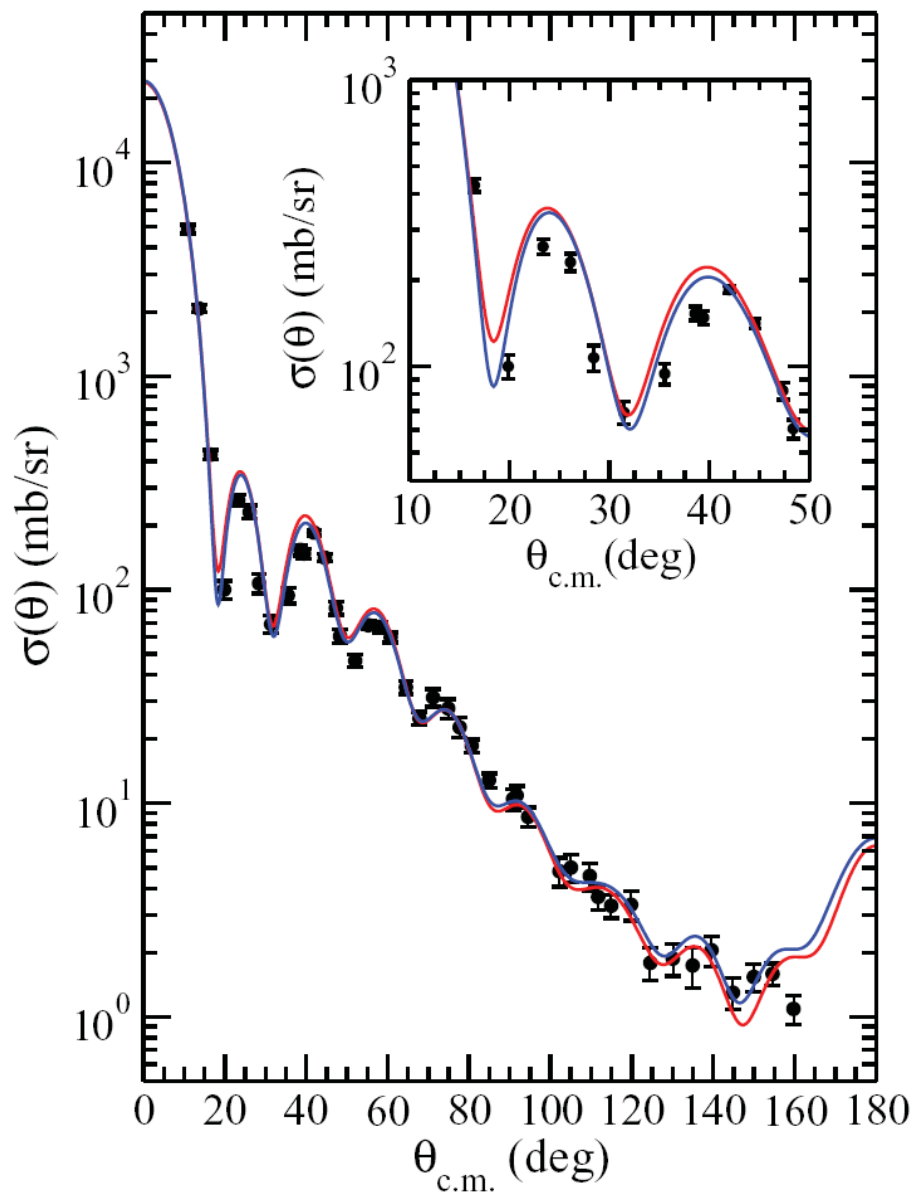


Fig. 3-5 (Color online) The  $^{209}\text{Bi}(n,n)$  data at 37 MeV (solid circles) compared to the nominal prediction of the global OM (at the back angles, the lower, red curve) and the modified version of the OM (blue curve), as described in the text. Both curves display the sum of elastic and inelastic cross sections.



## ***New DDX measurements of $^9\text{Be}$ at 8.19 MeV and 25.20 MeV***

The secondary neutron spectrum measurement with the multi-detector fast neutron TOF spectrometer at the HI-13 Tandem Accelerator at CIAE in 8.19 MeV and 21.94 MeV was performed. The neutrons were produced by the  $\text{D(d,n)}^3\text{He}$  and  $\text{T(d,n)}^4\text{He}$  reaction with a deuterium(tritium) gas target. The results were normalized to n-p scattering measurement. In the data reduction, a special Monte-Carlo code which was validated with the MCNP-4C code was employed to analyze the measured data for the corrections of neutron flux attenuation, multiple scattering and finite geometry. The measured DDXs were determined by comparing the simulated TOF spectra with the measured ones with an iterative procedure. The measured results were compared with the evaluated data and the other measurements.

The theoretical calculation was performed with the code LUNF which was based on the Hauser-Feshbach and the exciton model developed by CNDC. The DDX for  $^9\text{Be}$  induced by 21.94 MeV neutrons was calculated and compared with the experimental data. Proposals to improve the theoretical models were pointed out.

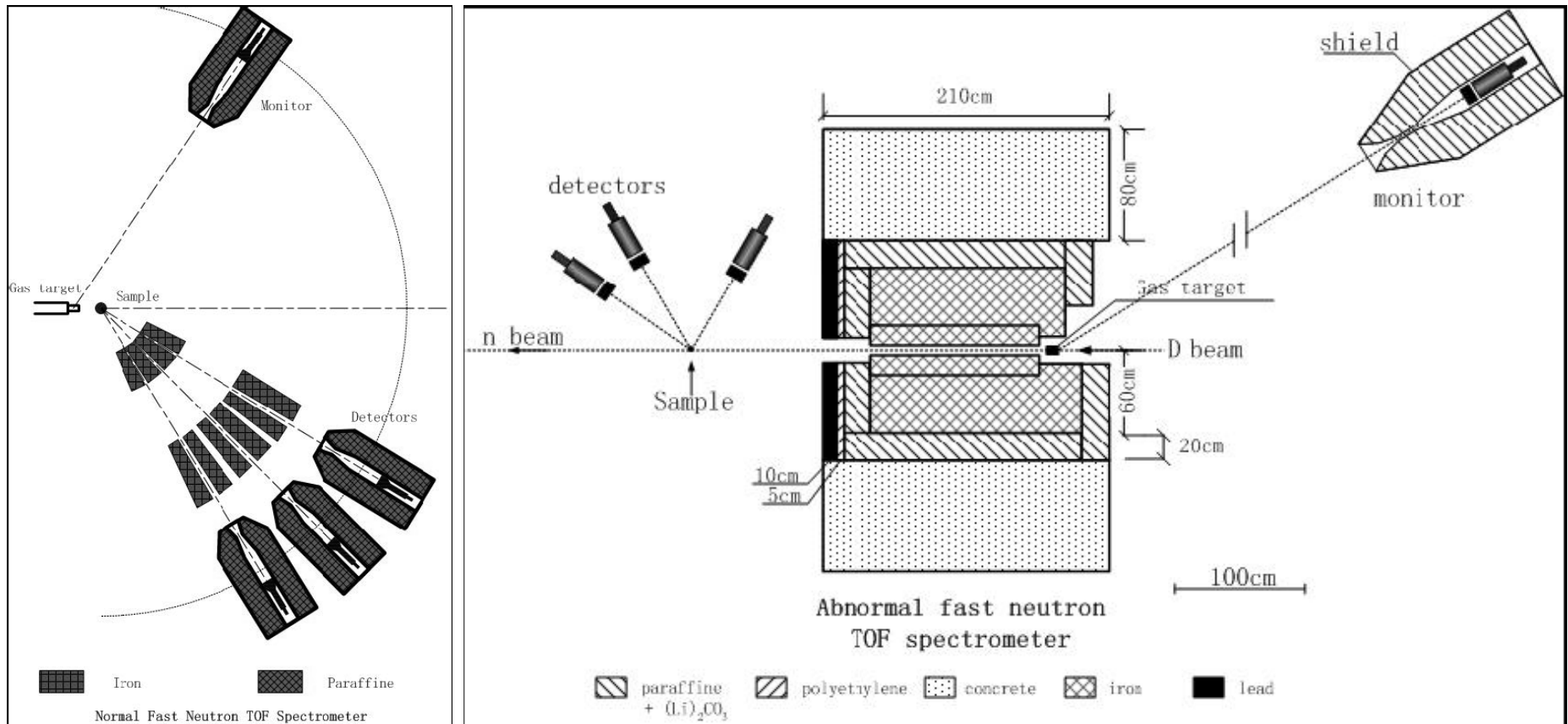


Fig. 3-6 Schematic view of normal(left) and abnormal(right) fast neutron and TOF spectrometer.

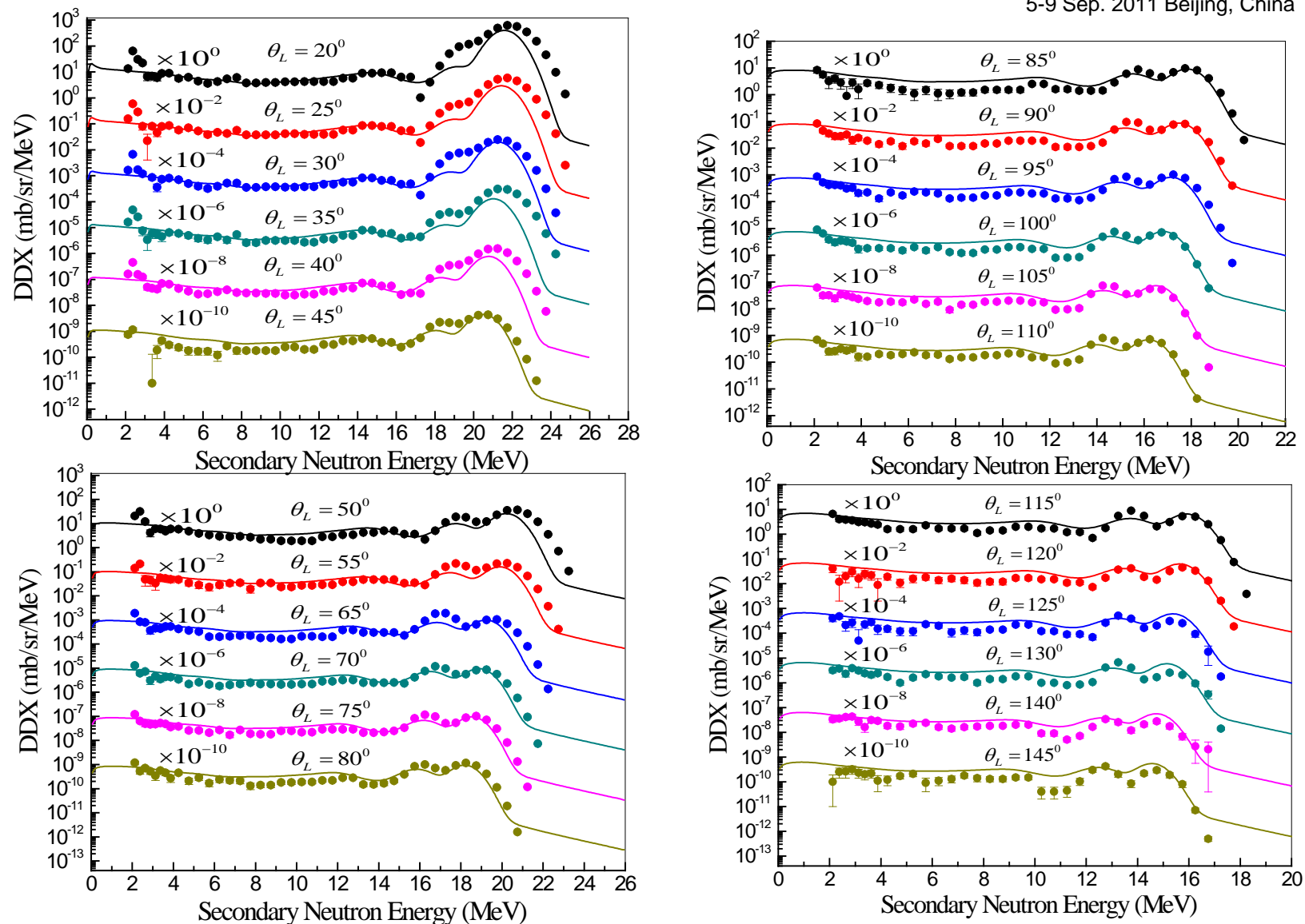


Fig.3-7 The experimental data compared with LUNF code calculated data.



## **4. Conclusions**

The most of nuclear data measurement activities performed in China Nuclear Data Coordination Network(CNDCN).

The re-evaluation and adjustment for some data files of CENDL-3.1 are continue doing according to the back feed after the end of 2009.

A series benchmark testing/validation for CENDL-3.1 performed at CNDC and some results of the testing/validation are used in the re-evaluation and adjustment process.

Relevant methodology studies are going on and some of are used for the evaluations of nuclear data file.

Some facilities are used for the neutron data measurements, although they are not in the good condition, and some good measured results obtained.

Some new facilities will be available for nuclear data experiments, and some facilities are under construction. .





***Thank you for your attention !  
Comments and suggestion welcome !***